EDGE EFFECTS IN STABILITY OF CUTS AND SLOPES IN COHESIVE SOILS

A Thesis Submitted
In Partial Fulfilment of the Requirements
for the Degree of
MASTER OF TECHNOLOGY

By
SUJIT KUMAR BHAKAT

to the

DEPARTMENT OF CIVIL ENGINEERING

INDIAN INSTITUTE OF TECHNOLOGY KANPUR

JANUARY, 1977

CERTIFICATE

This is to certify that the work presented in this thesis has been carried out by Mr. S.K. Bhakat under my supervision and has not been submitted elsewhere for a degree.

(YUDHBIR)
Professor
Department of Civil Engineering
Indian Institute of Technology, Kanpur

ACKNOWLEDGEMENT

I take this opportunity to express my deep sense of gratitude and profound regard to Dr. Yudhbir for his invaluable guidance and constant encouragement which was vital to the success of this effort.

I want to express my thanks to Mr. S. Ray and Mr. S. Mukhopadhyay for their whole hearted help particularly during the last stage of this work. Thanks are also due to my friends Messers A. Das, M. Patra, A. Nandi and K.K. Ray for their help from time to time. I am also thankful to my fellow users, the authorities and the staff of the Computer Centre at I.I.T. Kanpur for their help during the computational work.

Thanks are also due to Mr. J.C. Verma for the drawing work, Mr. V.K. Saxena and Mr. G.S. Trivedi for their neat and elegant typing.

SUJIT KUMAR BHAKAT

CONTENTS

LIST OF FIGURES

ABSTRACT

The overall problem of stability of unbraced vertical cuts and slope with horizontal ground surface is reviewed. Three-dimensional aspects of the problem are discussed in relation to factors controlling actual mechanism of stability.

$\phi = 0$ analysis is carried out to ascertain three-dimensional stability of vertical cuts and slopes in homogeneous saturated clay for two cases 1) strength constant with depth 2) Strength increasing with depth. Different composite geometrical failure surfaces are assumed and upper bound solution is minimised. Dimensionless stability charts incorporating three- dimensional aspects are presented and their usefulness in design of deep vertical cuts or slopes in saturated clays is discussed.

CHAPTER - I

INTRODUCTION

Overall stability problem of temporary unbraced vertical cuts and slopes with horizontal ground surface is of considerable economic significance as proper evaluation of factor of safety could result in appreciable savings in earthwork involved.

Much work has been done in the field of two dimensional analysis of factor of safety in which the main assumptions are that the failure length of the cut or slope is infinite and the soil is homogeneous. Most of these methods are based on limit equilibrium techniques.

However, for the problem like cuts and slopes having finite length, the conventional two dimensional analysis will give much lower factor of safety than the actual one in which the edge effects are also considered. At the edge portion of the failure zone, the radius of the shear surface will gradually decrease toward ends, which means that the shear surface is gradually shifted upward at the edges of failure and whose overall effect is to increase the factor of

safety of the cut or slope.

Most stability problems, related to man made or natural cuts, slopes and embankments are basically three dimensional. For cuts and slopes in normally consolidated clays and also compacted earth embankments, the short-term stability is of great concern. Therefore a $\phi = 0$ analysis has been carried out. As most two-dimensional stability analysis in the field is carried out for $\phi = 0$ condition, edge effects evaluated here would bring out reserve factor of safty available. This is basically a parametric study considering various factor influencing three-dimensional stability of cuts and slopes. The importance of evaluation of relevant strength characteristics to be used in any stability analysis, as brought out by Bjerrum (1973) is not considered here as the results of two dimensional and three-dimensional analyses are compared for same strength parameters. In this study the contribution of edge effects to the stability is brought out. Two strength variations with depth are considered.

i.e. 1) Strength constant with depth

2) Strength increasing with depth

For simplicity circular arc method is used and is extended to get three-dimensional factor of safety. The basic assumptions governing this method are retained except that the shear surface is now no more restricted to an infinitly long cylinder but is taken as a finite length of 2L. Three types of shear surfaces are considered.

1) Cylinder with planar edge surface
2) Cone attached to a cylinder
3) Ellipsoid attached to a cylinder

Results obtained from the analyses are represented in the form of dimensionless plots. From these plots one can easily find out the factor of safety of finite cuts or slopes considering the edge effects and the edge portion and cylindrical portion at failure in terms of the height of the slope.

CHAPTER - II

LITERATURE SURVEY

For any stability analysis, as the factor of safety depends very largely on the strength parameters used, they should be evaluated correctly. In this thesis this important aspect will not be discussed and reference should be made to an excellent paper on this topic (Bjerrum 1973). Many procedures, have been developed for plane strain slope stability analysis using limiting equilibrium techniques. All these procedures differ among themselves by the assumption made in order to achieve statical determinacy and the particular conditions of equilibrium that are satisfied.

Early investigations of quay wall failures led Swedish engineers to the conclusion that an appropriate stability analysis could be based on the assumption of circular failure surface. The most important advantage of the circular failure surfaces, is their significant simplification of the mechanics of slope stability analysis.

In 1918, Fellenius suggested a method, known as $\phi = 0$ method, for the analysis of short term stability of

slopes in homogeneous soil deposits. In this method the shear strength is treated entirely due to cohesion. The method of analysis is based on the consideration that, the sliding surface which requires the greatest amount of cohesion for equilibrium of the earth slope is the most dangerous one of all. The minimum value of F is found out by trial and error. The procedure consists of choosing several circular surfaces and picking out the surface which gives the minimum value of F.

$\phi = 0$ procedure is only applicable to the condition in which shear strength is independent of normal stress. For soils having both c and ϕ, the assumption of circular shear surface is insufficient to achieve statical determinacy. To achieve statical determinacy, log - spiral surface of the form $r = r_o e^{\theta \tan \phi}$ is choosen, where r is the radial distance of any point on the spiral from the centre point of the spiral, r_o is the reference radius and θ is the angle between r and r_o.

The main advantage of the spiral method is that the resultant of the normal stress and the frictional component of shear stress always passes through the centre of the spiral. So the moment equation will only involve the weight

force and the cohesive resistance of the soil.

Taylor (1937) has suggested a method for stability analysis of slopes in soil having both c and ϕ. The method is based on the consideration that, for a circular surface the resultant of the normal stress and the frictional component of shear resistance (R) will always lie tangent to a circle of radius r Sin ϕ, called the friction circle. But the summation of moments about the centre point will involve the normal stress distribution and because the unknown number of coefficients required to describe this distribution cannot be solved by three equations of equilibrium of statics, the problem is highly indeterminate.

To make the problem statically determinate it is assumed that the resultant (R) of the normal stress and the frictional part of the shear resistance is concentrated at a single point. This is equivalent to assuming that the normal stresses are concentrated at a single point. But for a reasonable distribution of normal stress along the shear surface the resultant normal force must be less than the scalar sum of its components. In order to produce the same moments as its components, R must lie tangent to a circle of greater radius than the friction circle. Taylor (1937)

has shown that the underestimate in the radius for the circle of tangency by the friction circle procedure is equivalent to using the correct radius for some assumed stress distribution with some what lower value of ϕ. If the magnitude and location of the resultant force due to normal and frictional shear stress component are assumed to be independent of normal stress distribution, then the equivalent value of ϕ_m may be calculated from the moment equation.

The underestimate in ϕ_m by friction circle analysis procedure may be represented by the ratio,

$$K = \frac{\text{Sin } \phi_m - \text{Sin } \bar{\phi}_m}{\text{Sin } \phi_m} \qquad (2.1)$$

where, ϕ_m is the mobilized friction angle corresponding to single concentrated force and $\bar{\phi}_m$ is the friction angle for some other assumed normal stress distribution. The value of K depends on the assumed normal stress distribution and the angle subtended by the shear surface at the centre.

Lambe and Whitman (1969) have shown that the assumption of two concentrated normal forces at each end of the shear surface gives an upper bound solution to the

factor of safety satisfying the three conditions of equilibrium. The solution is determinate since the magnitude of two normal forces and the factor of safety are the only unknowns to be calculated from the conditions of equilibrium.

All the methods described earlier are based on the equilibrium of the entire mass above the failure surface. There are many other methods in which the soil mass is devided into a number of slices and equilibrium of each slice is considered. The number of equations and unknowns associated with complete equilibrium of entire soil mass is summarized in table 1.

TABLE 1

EQUATIONS	
n	Moment equilibrium equations for each slice
n	Vertical force equilibrium equations for each slice
n	Horizontal force equilibrium equations for each slice
3n	Total equations

UNKNOWNS

1 - Factor of safety

n - Normal force on the base of each slice

n - Location of normal force on the base of each slice

n-1 - Interslice normal forces

n-1 - Interslice shear forces

n-1 - Location of interslice forces

5n-2 Total unknowns

The unknown normal force locations on the base of each slice may be eliminated from the equation of overall moment equilibrium by considering circular shear surface.

This equation may be written as -

$$\sum_{1}^{n} w.r. \operatorname{Sin}\alpha - \sum_{1}^{n} s\,\Delta l \; r = 0 \qquad (2.2)$$

where, w is the weight of individual slice,

r is the radius of failure surface,

α is the base slope of the slice, and

n is the total number of slices.

Substituting $s = c' + (\sigma - u) \tan \phi'$ (2.3)

$$F = \frac{\sum_{1}^{n} c' \; l + (N - u\Delta l) \tan \phi'}{\sum_{1}^{n} w \sin \alpha} \qquad (2.4)$$

in which 'Δl' is the length of the base of a particular slice. Assumption made in this formulation is that the normal force 'N' and the weight force 'W' act through a point at the centre of the base of each slice.

Fellenius (1927) suggested a method with an additional assumption that the interslice forces have zero resultant in the direction normal to the failure arc of that slice. With this assumption the normal force 'N' can be represented by

$N = W \cos \alpha$. (2.5)

Substituting this in equation (2.4)

$$F = \frac{\sum_{1}^{n} c\Delta l + (w \cos \alpha - u\Delta l) \tan \phi}{\sum_{1}^{n} w \sin \alpha} \qquad (2.6)$$

This procedure provides a direct means of calculating the factor of safety from the equations of overall moment

equilibrium, however neither force nor moment equilibrium is satisfied for the individual slice. In this method the assumptions regarding side forces involves n-1 equations where there are only n-2 unknowns. Hence the system of slice is overdeterminate and in general it is not possible to satisfy statics. Thus the factor of safety computed by this method will have error.

When the entire slope is in cohesive soil and it is appropriate to use undrained strength throughout the slope, then the equation (2.6) becomes greatly simplified. For a circular shear surface, this equation becomes

$$F = \frac{\sum_{i=1}^{n} s_u \Delta l_i}{\sum_{i=1}^{n} w_i \operatorname{Sin} \alpha_i} \qquad (2.7)$$

If the undrained strength is constant throughout the soil, then the numerator is simply $s_u \cdot l_a$ where l_a is the arc length of the failure surface. Taylor (1948) has produced some charts in which $s_u/\gamma'_t H$ values are plotted against depth factor D for different values of slope angle, where D is given by

$$D = \frac{H + H_T}{H} \qquad (2.8)$$

Here, H_T is the depth of soil below the toe of the slope and H is the height of the slope

Knowing D and slope angle, mobilized shear stress required for equilibrium can easily be found out from these charts.

Spencer (1967) has described a procedure for satisfying complete slice equilibrium for a circular shear surface. Assuming that the normal forces are located at the centre of the base of each slice, Spencer achieved statical determinacy with the additional assumption that all resultant interslice forces are parallel. The (n-1) unknown side force inclinations are thereby replaced by a single unknown inclination, resulting into 3n unknowns. Although the solution presented by Spencer was only directly applicable to a circular shear surface, his procedure may be extended to slip surface of any shape.

Bishop (1955) has presented a method with assumptions that normal force and weight force act through the mid-point of the base of each slice and the interslice forces have zero resultant in vertical direction. With these assumptions,

factor of safety was given by

$$F = \frac{\sum_{i=1}^{n} \bar{c}\,\Delta x_i + (w_i - u_i \Delta x_i) \tan \phi \; \frac{1}{M_i(\alpha)}}{\sum_{i=1}^{n} w_i \operatorname{Sin} \alpha_i} \qquad (2.9)$$

where, $M_i(\alpha) = \operatorname{Cos} \alpha_i \left[1 + \frac{\tan \phi' \tan \alpha_i}{F}\right]$, (2.10)

α_i is the base angle of ith slice,

Δx_i is the width of ith slice,

and u_i is the pore pressure at the base of ith slice

Whitman and Bailey (1967) have shown that numerical difficulties may arise in the use of Bishop's procedure when deep failure surfaces are analysed. In this case, the angle α may have large negative values such that $1/M_i(\alpha)$ is zero or negative resulting in the normal force at the base of the slice being very large or negative, a situation implying an unreasonable stress state. Whitman & Bailey have indicated that, if the value of

$$\left(1 + \frac{\tan \phi \tan \alpha_i}{F}\right)$$

for any slice is less than 0.2 the solution should be rejected

Morgenstern and Price (1965, 1967) have presented a some what different approach to the solution of complete slice equilibrium. The assumption made by Morgenstern and Price is that the shear and normal forces between the slices are related by the expression

$$X_j = \lambda f(x) E_j \qquad (2.11)$$

where the assumed function f(x) represents the variational relationship between the normal and shear component of forces (E_j, and X_j respectively) between the slices. The parameter λ is an unknown factor defining the relation between X and E in terms of f(x). By assuming f(x) the (n-1) values of X are replaced by the single unknown. Even with this assumption n additional assumptions are required for statical determinacy. These additional assumptions are achieved in Morgenstern and Price procedure by assuming that f(x) varies linearly between each interslice boundary at which its values are specified. By assuming this variation for f(x), the location of normal forces on the base of each slice are thus fixed. So the total number of unknowns are 3n.

Gibson and Morgenstern (1962) suggested a method

for stability analysis of cuttings in normally consolidated clays in which the strength increases with depth. They established an expression for factor of safety, based upon $\phi = 0$ analysis, assuming that the soil strength varies linearly with depth, as

$$F = N - \frac{c}{\gamma z}$$

where N is stability number, which depends upon the slope geometry.

Many other procedures are available for slope stability analysis (Janbu, Lowe & Karafaith, Janbu's Generalized procedure of slice, Seed and Sultan etc.). From the investigation of homogeneous slopes, the conclusions may be drawn with regards to the accuracy of the various analysis procedures as

1) Janbu's Generalized procedure of slice and Spencer's procedure appear to give very similar results and are probably the most accurate procedures.

2) The values of factor of safety calculated by the Morgenstern and Price procedure would be at least as accurate as the values calculated using either Janbu's Generalized procedure of slice or Spencer's procedure.

3) The log-spiral procedure gives results which are equally comparable to those by the procedures of Janbu and Spencer, however, so far analyses using the log-spiral have only been conducted for zero pore pressure cases.

4) The modified Bishop procedure results in slightly lower factors of safety than either the generalized procedure of slice, Spencer or log-spiral procedures. The difference appears to be less than 4% for values of 'r_u' as large as 0.6.

5) The values of factor of safety calculated using any of the above procedures with 'r_u' = 0, are generally from $1\frac{1}{2}\%$ to $3\frac{1}{2}\%$ higher than the lower bound equilibrium values calculated by friction circle method.

6) The values of the factor of safety calculated by the ordinary method of slices are generally from $1\frac{1}{2}\%$ to $3\frac{1}{2}\%$ less than the lower bound equilibrium values and as much as $6\frac{1}{2}\%$ lower than more accurate values calculated by procedure like Modified Bishop. These differences correspond to analyses without pore pressures. For analyses

with pore pressure even larger errors will result by using the ordinary method of slices.

In contrast to the voluminous literature on two dimensional slope stability, very little work has been done regarding three dimensional problems. Sherard et.al. (1963) present a method for three-dimensional analysis, particularly in case of high dams in narrow valleys, in which the length of the dam is devided into a series of segments of equal length and the average cross-section of each segment is analysed as 2-D problem. The factor of safety is then defined as the ratio of the sum of resisting forces to the sum of the driving forces for all segments of dam length. The result of this calculation essentially gives a 'weighted' average of the stability of the various sections of the embankment.

Yudhbir and Varadarajan (1975) have analysed the Beas dam foundation as a three-dimensional problem. Due to the nature of shear zones present in the bed rock, the dam along its length consisted of blocks of variable resistance. Lateral resistance between stable and unstable blocks was evaluated to compute three-dimensional factor of safety. This is an effective stress approach and the main difficulty in

adopting effective stress approach is the uncertainty about the status of lateral stress on edges and the relevant strength parameters to be used in the analysis.

Baligh and Azzouz (1976) extended the concept of two dimensional circular arc method to three dimensional stability problems, in which some function g(z) is assumed to represent the failure surface. The whole length of the failure is devided into a number of segments, each of them having very small thickness. All the segments are then analysed seperately as 2-D problem. Then the 3-D factor of safety is represented by the ratio of the sum of the resisting moments to the sum of the driving moment, for all segments in the failure length.

Bhandari (1970) suggested a method for stability analysis of mud flows considering the edge resistance. In this method the normal force on the plane of shearing is found out by

i) the application of the concept of earth pressure calculation

ii) the possible principal shear distribution on the side boundary shear.

Basal resistance is found out by Morgenstern & Price (1965, 1967) or by Janbu et.al. (1956) or by the conventional method. The total resistance mobilized against sliding is expressed in terms of the factor of safety F, which is then evaluated by comparing the mobilised resistance with the gravity produced shearing forces. It is shown that edge effects are of the order of 18%.

Statement of Problem :

In this thesis an approach similar to the one adopted by Baligh & Azzouz (1976) will be adopted to investigate edge effects in slope stability analysis. Different types of admissible edge surfaces will be investigated to obtain an upper bound solution. Cases of constant and variable strength with depth will be investigated.

CHAPTER III

METHOD OF ANALYSIS

3.1 Two Dimensional Analysis:

Before proceeding with three-dimensional analysis, the minimum plane-strain factor of safety, critical centre of rotation and the shear surface giving the minimum factor of safety (2-D) is to be found out. For simplicity circular arc method has been used to get minimum factor of safety and the analysis is carried out for two cases:

1) Constant strength
2) Strength increasing with depth

Case-1:

The expression for driving moment per unit length is given (Taylor 1937) as:

$$M_d^o = \frac{\gamma H^3}{12} \left(1-2 \cot^2 \beta + 3 \cot\lambda \cot\beta + 3 \cot\alpha \cot\lambda - 3 \cot\alpha \cot\beta \right) \qquad (3.1.1)$$

The expression for resisting moment per unit length is:

$$M_r^o = 2\alpha \cdot R^2 \cdot c \qquad (3.1.2)$$

where, α , β , λ are as shown in Fig. 3.1a

and γ is the unit weight of soil.

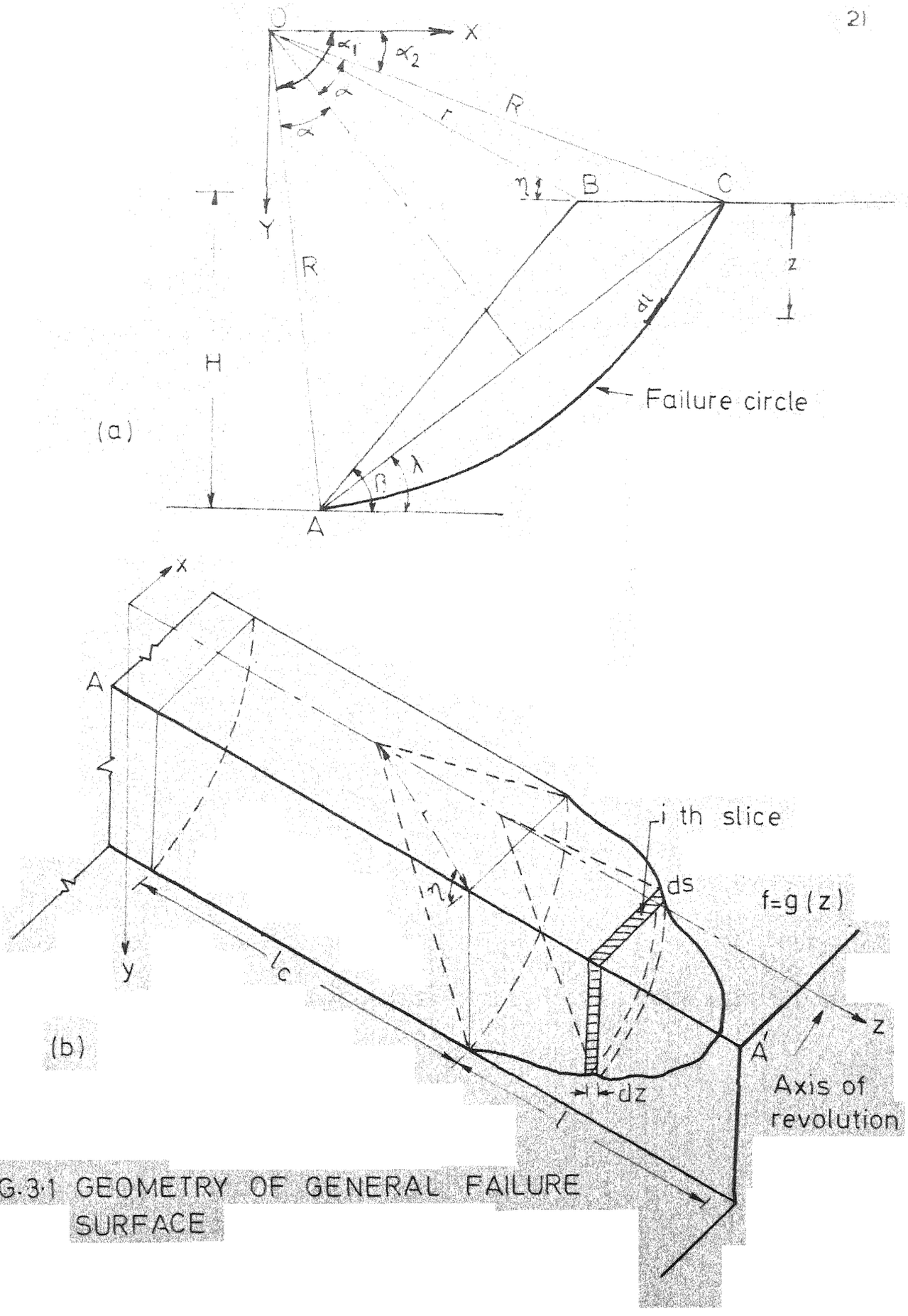

FIG. 3.1 GEOMETRY OF GENERAL FAILURE SURFACE

H is the height of the slope or vertical cut

c is the avarage undrained strength of the soil.

So the two-dimensional factor of safety can be given by:

$$F_o = \frac{M_r^o}{M_d^o} \qquad (3.13)$$

Case-2:

This case has been discussed by Gibson and Morgenstern (1962). The strength at any depth z can be represented by:

$$c = \frac{kz}{H} \qquad (3.1.4)$$

From Fig. 3.1, the resisting moment for small length dl at depth z on the shear surface is given as:

$$d M_r^o = R \cdot dl \cdot c$$

where, $dl = R\, d\theta$

$$\therefore \quad dM_r^o = R^2 d\theta \frac{kz}{H} \qquad (3.1.4a)$$

where $z = R \sin\theta - R \sin \alpha_1$

Substituting the value of z in equation (3.1.4a).

$$dM_r^o = \frac{R^3 k}{H} (\sin\theta - \sin\alpha_1)\, d\theta$$

Hence, $$M_r^o = \frac{R^3 k}{H} \int_{\alpha_1}^{\alpha_2} (\sin\theta - \sin\alpha_1)\, d\theta$$

$$\text{or,} \quad M_r^o = \frac{kR^3}{H} \left[\text{Cos}\alpha_2 - \text{Cos}\alpha_1 - \text{Sin}\alpha_1 \, (\alpha_2 - \alpha_1) \right]$$

From Fig. 3.1 , it is clear that :

$$\alpha_2 - \alpha_1 = 2\alpha$$

$$R \, \text{Sin}\, \alpha_1 = R \, \text{Cos}\alpha \, \text{Cos}\, \lambda - R \, \text{Sin}\, \alpha \, \text{Sin}\lambda$$

$$R \, (\text{Cos}\alpha_2 - \text{Cos}\, \alpha_1) = H \, \text{Cot}\lambda$$

and , $H = 2 R \, \text{Sin}\alpha \, \text{Sin}\lambda$

$$M_r^o = \frac{kR^2}{H} \left[H \, \text{Cot}\lambda - 2\alpha R \, (\text{Cos}\alpha \, \text{Cos}\lambda - \text{Sin}\, \alpha \, \text{Sin}\lambda) \right]$$

$$= \frac{kH^2}{4 \, \text{Sin}^2 \alpha \, \text{Sin}^2 \lambda} \left[\text{Cot}\lambda + (1 - \text{Cot}\alpha \, \text{Cot}\lambda) \, \alpha \right] \qquad (3.1.5)$$

Where as the expression for driving moment remains same as given by Equation (3.1.1). The 2-D factor of safety may now be given as:

$$F_o = \frac{\left[\text{Cot}\lambda + (1 - \text{Cot}\alpha \, \text{Cot}\lambda) \, \alpha \right]}{\text{Sin}^2 \alpha \, \text{Sin}^2 \lambda \left[1 - 2 \, \text{Cot}^2 \beta + 3 \, \text{Cot}\alpha \, \text{Cot}\beta + 3 \text{Cot}\alpha \, \text{Cot}\lambda \right.}$$

$$\left. - 3 \, \text{Cot}\alpha \, \text{Cot}\, \beta \right] \cdot \frac{3c}{\gamma z} \qquad (3.1.6)$$

$$\text{or,} \quad F_o = N . \frac{c}{\gamma z} \qquad (3.1.7)$$

For normally consolidated clay, $c/\gamma z$ is constant for a particular soil. So minimization of N is needed to obtain

least value of F_o.

Repeated trials have been made to obtain least value of F_o (i.e. F_{omin}) for both the cases and these are performed by means of a computer programme (Appendix A). R represents the radius of the failure surface corresponding to F_{omin} and (r, η) represents the position of the centre of rotation as shown in the Fig. 3.1a.

For a cut of 6 meter deep in soil ($\gamma = 1.77$ t/m^3) having constant strength with depth, the minimum two-dimensional factor of safety is obtained as $F_{omin} = 1.56741$

Radius of the critical circle R = 16.25 meter

$\eta = 41.0^o$

r = 11.52 meter

For a 9 meter deep cut in soil where strength is increasing with depth (k = 6.85 t/m^2, γ = 1.6 t/m^3) the minimum two-dimensional factor of safety is found as :

F_{omin} = 0.933

R = 586 meters

η = 45^o

r = 580 meters

In this case, the failure surface becomes almost a planar surface.

3.2 Three-Dimensional Analysis:

Vertical cut:

Getting all these values from two-dimensional analysis, one can proceed to perform three-dimensional analysis.

Let the function $f = g(z)$ represents the failure surface of revolution at the edge, which is symmetric about an axis (z-axis) through the critical centre and parallel to the length of the slope (Fig. 3.1b). Now the three-dimensional factor of safety can be written as:

$$F^* = \frac{M_r^o \cdot 2\, l_c + \text{Resisting moment at the edges}}{M_d^o \cdot 2\, l_c + \text{Driving moment at the edges}} \qquad (3.2.1)$$

where, M_r^o is the resisting moment per unit length corresponding to the critical circle, M_d^o is the driving moment per unit length corresponding to the critical circle and l_c is the half of the length of the cylindrical portion of the failure mass.

To start three-dimensional analysis, it is necessary to decide the location of the axis of rotation and the type of an edge surface which will minimise the three-dimensional factor of safety. In this analysis, a

rigid body motion of the entire failure mass (cylindrical and edge portions) is assumed about a linear axis of rotation.

The critical centre and surface as found by two-dimensional analysis have been assumed applicable for three-dimensional analysis also. Two types of edge surfaces, namely, conical and ellipsoidal are considered and critical values for planar and spherical edge surfaces for a given geometry of cut are also investigated. In the first case the surface of revolution becomes a cylinder attached to a cone and in the second case it becomes a cylinder attached to an ellipsoid.

Considering symmetry of the failure zone about z = 0 plane (Fig. 3.1b), let l_c be the length of the cylindrical portion on one side of the failure zone and l be the length of the edge portion. The length of the cylindrical and edge portion (l_c and l) are measured along a line which lies on the surface of the slope at shortest distance from the axis of rotation of the sliding mass. The position of the line along which maximum length of failure occurs will also depend on the position of the axis of rotation (η , r). For a vertical cut the value of η lies between 40^o to 45^o for both the cases (i.e. constant strength and strength

increasing with depth). From Fig. 3.1a it is seen that point B on the surface of the slope is at shortest distance(r) from point O.

In the case of a vertical cut, maximum length of failure will be measured along a line through B (Fig. 3.1a) in the direction perpendicular to the plane of the paper (i.e. along the line of intersection of top horizontal plane and the vertical plane).

For computation purposes, the edge portion of the failure mass is devided into 'n' number of slices, each having very small thickness dz, such that $n = l/dz$. Now it is needed to represent all the geometrical parameters associated with ith slice in terms of known parameters l, R, r and η. This needs to be done for both types of edge surfaces.

Conical Edge Surface:

Consider z-axis as the line through the critical centre obtained from 2-D analysis and parallel to the length of the slope. X-axis is shown in Fig. 3.2c. Let C_1 be the height of the cone. Now in the plane zox' equation of line $x_o' z_o$ (Fig. 3.2 a) is given by:

$$\frac{x'}{C_1 - z} = \frac{R}{C_1}$$

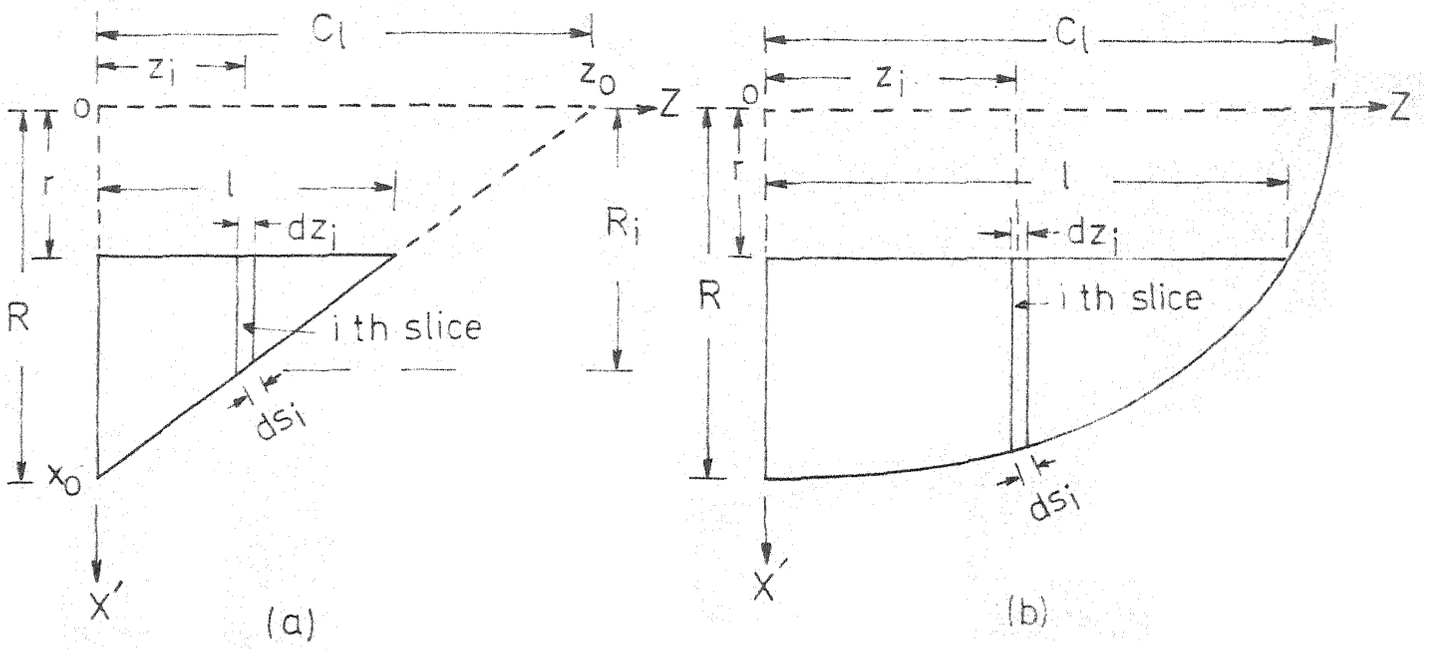

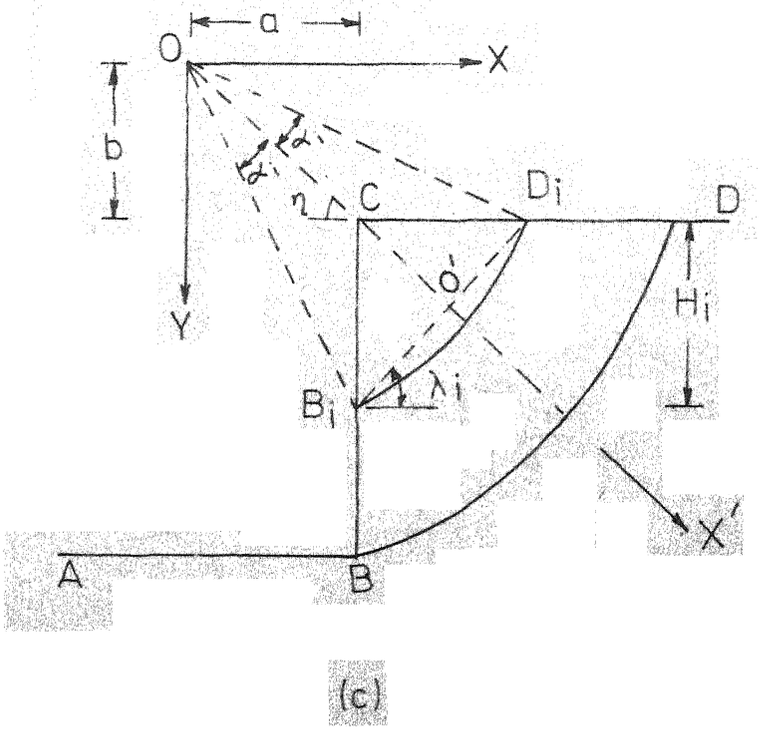

FIG. 3·2 SPECIFICATION OF PARAMETERS

$$x' = R - \frac{Rz}{C_1} \qquad (3.2.2)$$

$$\frac{dx'}{dz} = -\frac{R}{C_1}$$

$$ds_i = \sqrt{1 + \frac{R^2}{C_1^2}}\, dz$$

or, $$ds_i = \frac{dz}{C_1} (C_1^2 + R^2)^{1/2} \qquad (3.2.3)$$

C_1 can be found out from the boundary condition.

At $x' = r$, $z = l$ (where l is the failure length at the edge).

From equation (3.2.2):

$$r = R - \frac{Rl}{C_1}$$

$$\therefore \quad C_1 = \frac{lR}{(R-r)} \qquad (3.2.4)$$

In Fig. 3.2a let z_i be the distance of the middle plane of ith slice from x' axis :

then, $z_i = (2i - 1)\frac{dz}{2}$.

Radius of the circle confining the ith slice can be found out from equation (3.2.2)

$$\text{i.e. } R_i = R - \frac{R \cdot z_i}{C_1} \qquad (3.2.5)$$

Elliposoidal Edge:

With orientation of the z and x' axes same as in the previous case, the equation of the ellipse in x'oz plane (Fig. 3.2b) is given by:

$$\frac{x'^2}{R^2} + \frac{z^2}{C_1^2} = 1 \qquad (3.2.6)$$

$$\therefore x'^2 = \left(1 - \frac{z^2}{C_1^2} \right) R^2$$

$$\text{Or,} \quad x' = \left(1 - \frac{z^2}{C_1^2} \right)^{1/2} R$$

$$\frac{dx'}{dz} = - \frac{R}{C_1 \sqrt{\left(C_1^2 - z^2 \right)}}$$

$$\therefore ds_i = \sqrt{1 + \frac{R^2}{C_1^2} \frac{z_i^2}{\left(C_1^2 - z_i^2 \right)}} \, dz \qquad (3.2.7)$$

where, $z_i = (2i - 1) \frac{dz}{2}$.

C_1 can be found out from the condition that , when:

$x' = r, \quad z = l$

Hence from equation (3.2.6):

$$\frac{r^2}{R^2} + \frac{l^2}{C_1^2} = 1$$

$$\therefore C_1^2 = \frac{l^2 R^2}{R^2 - r^2} \quad ;$$

$$\text{or,} \quad C_1 = \frac{l\,R}{(R^2 - r^2)^{1/2}} \qquad (3.2.8)$$

Let the radius of the circle confining the ith slice be R_i.

Hence at $z = z_i$, $x' = R_i$

From equation (3.2.6):

$$R_i^2 = R^2 \left(1 - \frac{z_i^2}{C_1^2} \right)$$

$$\text{or,} \quad R_i = \frac{R}{C_1} \sqrt{(C_1^2 - z_i^2)} \qquad (3.2.9)$$

For known values of R and r (obtained from 2-D analysis) and for a particular value of l, C_1 can be found out from equations (3.2.4) and (3.2.8) for two types of edge surfaces. Knowing R_i (Equations 3.2.5 and 3.2.9) one can proceed to evaluate other parameters , H_i, λ_i , α_i (Fig.3.2c). Now the equation of the circle confining the ith slice with respect to x and y axis is:

$$x^2 + y^2 = R_i^2 \qquad (3.2.10)$$

Equation of line BC (from Fig. 3.2c) is :

$$x = a$$

$$\therefore \quad y = (R_i^2 - a^2)^{1/2} \quad \text{(Taking only positive value)}$$

$$H_i = y - b = (R_i^2 - a^2)^{1/2} - b \qquad (3.2.11)$$

where, $a = r \cos\eta$ (3.2.12a)

$b = r \sin\eta$ (3.2.12b)

From Fig.3.2c.

$$\alpha_i = \frac{1}{2}.(\angle B_i o\, x - \angle D_i\, o\, x)$$

$$\sin \angle B_i ox = \frac{H_i + b}{R_i}$$

or $$\angle B_i ox = \sin^{-1}\left(\frac{H_i + b}{R_i}\right)$$

Similarly,

$$\angle D_i ox = \sin^{-1}(b/R_i)$$

$$\therefore \quad \alpha_i = \frac{1}{2}\left[\sin^{-1}\left(\frac{H_i + b}{R_i}\right) - \sin^{-1}(b/R_i)\right] \qquad (3.2.13)$$

Again from triangle $OO'B_i$

$$o'B_i = oB_i \sin \alpha_i$$

$$= R_i \sin \alpha_i$$

$$B_iD_i = 2\, o'B_i = 2 R_i \sin\alpha_i$$

$$\therefore \lambda_i = \sin^{-1}\left(\frac{H_i}{B_iD_i}\right) = \sin^{-1}\left(\frac{H_i}{2 R_i \sin\alpha_i}\right) \qquad (3.2.14)$$

Driving and Resisting Moments:

Case I:

Knowing all these values one can represent the expression for driving moment for ith slice as :

$$M^{o}_{di} = \frac{\gamma H_i^3}{12} \left[1+3 \cot\alpha_i \cot\lambda_i\right] \quad dz \qquad (3.2.15)$$

Expression for resiting moment for ith slice, considering constant strength is:

$$M^{o}_{ri} = 2\, \alpha_i\, R_i^2 \cdot c \cdot ds_i \qquad (3.2.16)$$

where, c is the strength of the soil.

Case II:

Expression for resisting moment for ith slice in the second case (i.e. strength increasing with depth) is:

$$M^{o}_{ri} = \frac{k\, H_i^2}{4 \sin^2\alpha_i \sin^2\lambda_i} \left[\cot\lambda_i + \alpha_i(1-\cot\lambda_i \cot\alpha_i)\right] ds_i \qquad (3.2.17)$$

In this case also the expression for driving moment can be represented by equation 3.2.15. So finally three- dimensional factor of safety can be given by:

$$F^* = \frac{M^{o}_{r} \cdot l_c + \sum_{i=1}^{n} M^{o}_{ri}}{M^{o}_{d} \cdot l_c + \sum_{i=1}^{n} M^{o}_{di}} \qquad (3.2.18)$$

Slopes:

In case of slopes in parely cohesive soil, the failure length may not always attain maximum value along the line of inter section of top horizontal plane and the sloping plane, but it may be maximum along any line on the surface depending on the position of axis of rotation (Fig.3.3). Maximum length of failure will be measured along a line which lies on the surface of the slope and at shortest distance from the axis of rotation.

From Fig. 3.4 a it can be concluded that if $\varphi + \beta < 90^{o}$ then the point S on the surface of the slope will be at shortest distance from '0' and consequently the failure length will attain maximum value along the line through S and parallel to the axis of rotation of the failure mass (i.e. the projection of the axis of rotation on the inclined face of the slope).

If $90 + \beta \geq \varphi + \beta \geq 90$, then the failure length will attain maximum value along the crest of the slope (i.e. line through C and parallel to the axis of rotation). Let u be the distance from the axis of rotation of the line along which maximum length will be attained. In the first case u = OS and in the second case u = OC. Procedure for

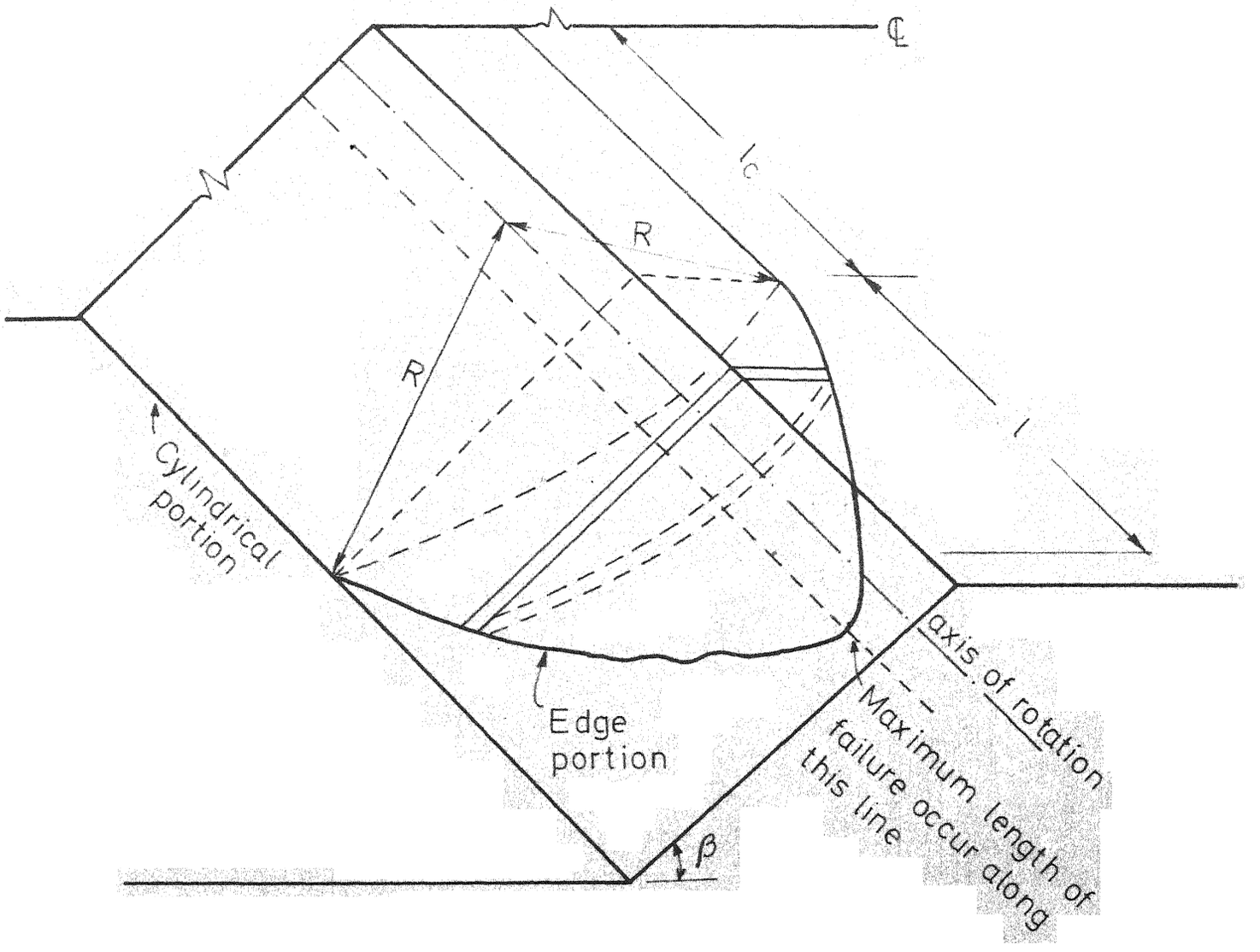

FIG.3·3 GEOMETRY OF GENERAL FAILURE SURFACE (SLOPES)

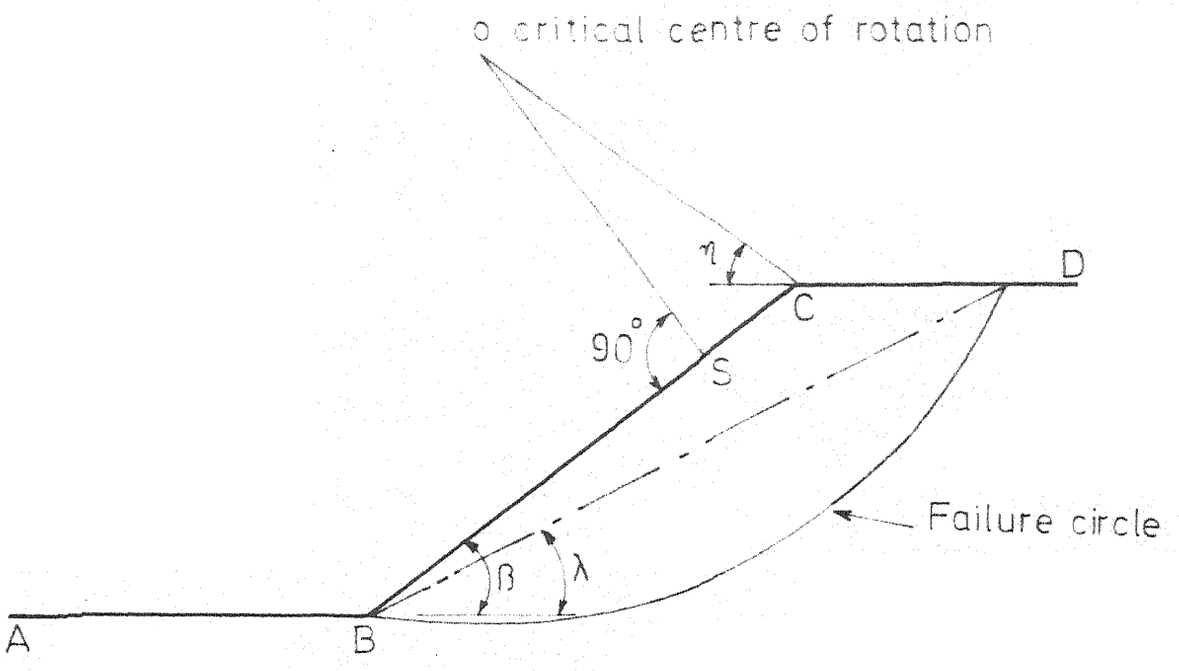

(a)

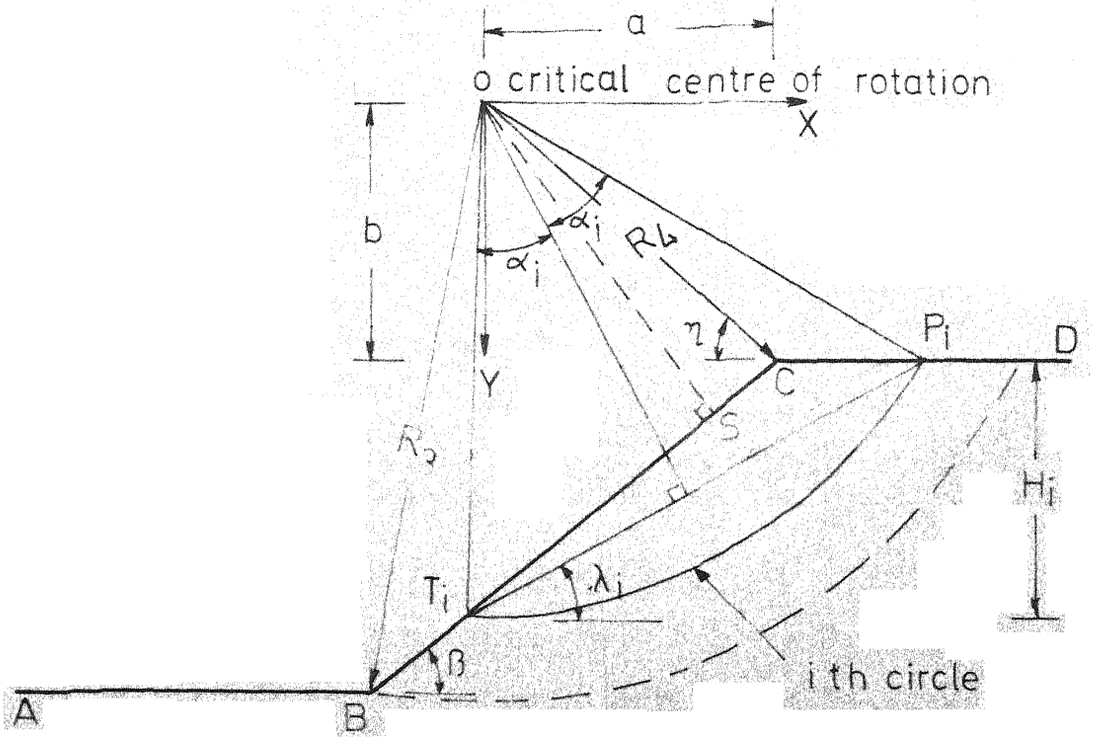

(b)

FIG·3·4 SPECIFICATION OF PARAMETERS

analysing the slopes remains same as for vertical cuts except that the expression for different parameters, driving and resisting moments are to be modified for both type of edge surfaces (i.e. conical and ellipsoidal).

Conical Edge:

As before, let z_i is the distance of the middle plane of ith slice from the end of the cylindrical portion, so,

$$z_i = (2 i - 1) \frac{dz}{2}$$

and, $$ds_i = \frac{dz}{C_1} \sqrt{C_1^2 + R^2}$$

where, $$C_1 = 1 R / (R-u) \qquad (3.2.19)$$

Radius of the ith slice is:

$$R_i = R - \frac{R z_i}{C_1}$$

Ellipsoidal Edge:

Here also the expressions for ds_i , C_1 and R_i will remain same as in the case of vertical cut.

$$ds_i = 1 + \sqrt{\frac{R^2}{C_1^2} \cdot \frac{z_i^2}{C_1^2 - z_i}} \quad dz$$

$$C_1 = \frac{1R}{R^2-u^2} \qquad (3.2.20)$$

and the radius of the ith slice:

$$R_i = \frac{R}{C_1} \sqrt{(C_1^2 - z_i^2)}$$

Knowing R_i and C_1, other geometric parameters can be found out. Equation of the circle confining the ith slice can be given by the equation (3.2.10) i.e.:

$$x^2 + y^2 = R_i^2$$

Equation of line BC (Fig. 3.4b) is given by:

$$y = - x \tan\beta + (b + a \tan\beta)$$

or
$$y = (a - x) \tan\beta + b \qquad (3.2.21)$$

$$x = a - (b - y) \cot\beta$$

Putting this expression of x in equation (3.2.10) the following equation is obtained:

$$(b-y)^2 \cot^2\beta + a^2 - 2a (b-y) \cot\beta + y^2 = R_i^2 \qquad (3.2.22)$$

This is a quadratic equation in y whose two roots y_T and y_h are as follows:

$$y_T = \frac{A + \sqrt{B}}{\mathrm{Cosec}^2\beta} \qquad (3.2.23a)$$

$$y_h = \frac{A - \sqrt{B}}{\text{Cosec}^2\beta} \qquad (3.2.23b)$$

where,

$$A = \text{Cot}\beta\,(a + b\,\text{Cot}\beta) \qquad (3.2.23c)$$

$$B = R_i^2\,\text{Cosec}^2\beta - (b\,\text{Cot}\beta - a)^2 \qquad (3.2.23d)$$

From Fig.3.4b it is evident that when R_i is less than R_4, i.e. OC > OS, then both the toe and the heel of failure circle will lie on the line BC. Again when $R_3 > R_i > R_4$, then the toe of the failure circle will lie on line BC, whereas the heel will lie on line CD. Similarly for $R_i > R_3 > R_4$, the toe of the failure circle will lie on line AB and the heel will lie on line CD. Here all the geometric parameters are evaluated for the above mentioned cases.

Case a:

$$R_i < R_4$$

Here both the toe(T_i) and heel (P_i) of the ith failure circle will lie on line BC.

From the Fig. 3.4b it is seen that :

$$H_i = y_T - y_h$$

Where y_T and y_h are given by equations (3.2.23a) and (3.2.23b) respectively.

Hence, $$H_i = \frac{2\sqrt{B}}{\text{Coec}^2\beta} \qquad (3.2.24a)$$

In this case the chord T_iP_i is lying on line BC,

$$\lambda_i = \beta \qquad (3.2.24b)$$

Chord length $T_iP_i = \dfrac{H_i}{\sin \lambda_i} = H_i \operatorname{Cosec} \beta$

$$\alpha_i = \sin^{-1}\left(\frac{T_iP_i}{2R_i}\right) = \sin^{-1}\left(\frac{H_i \operatorname{Cosec}\beta}{2R_i}\right) \qquad (3.2.24c)$$

Case b:

$$R_3 > R_i > R_4$$

In this case as the heel of the ith failure circle is lying on line CD, the ordinate of the heel point can be given by, $y_h = b$. From Fig. 3.4b:

$$H_i = y_T - y_h = y_T - b$$

$$= \frac{A + \sqrt{B}}{\operatorname{Cosec}^2\beta} - b$$

$$= \frac{(a \cot\beta - b) + R_i^2 \operatorname{Cosec}^2\beta - (b\cot\beta - a)^2}{\operatorname{Cosec}^2\beta} \qquad (3.2.25a)$$

The equation of line CD can be given by y=b. Substituting this in equation (3.2.10):

$$x = x_h = (R_i^2 - b^2)^{1/2} \qquad (3.2.25b)$$

Here only the positive value of x is taken since the x-co-ordinate of heel of ith failure circle can not be

negative. So the co-ordinate of point P_i is (x_h, y_h).

Substituting in equation (3.2.21):

$$x_T = -(y_T - b)\,\mathrm{Cot}\,\beta + a$$

$$= a - H_i\,\mathrm{Cot}\,\beta \qquad (3.2.25c)$$

So the chord length T_iP_i is:

$$T_iP_i = (x_h - x_T)^2 + (y_h - y_T)^2$$

Hence, $$\lambda_i = \mathrm{Sin}^{-1}\left(\frac{H_i}{T_iP_i}\right) \qquad (3.2.25d)$$

and, $$\alpha_i = \mathrm{Sin}^{-1}\left(\frac{T_iP_i}{2\,R_i}\right) \qquad (3.2.25e)$$

Case c:

$$R_i > R_3 > R_4$$

Here the toe point (T_i) of ith failure circle will lie on line AB, whereas the heel point (P_i) will lie on line CD. So, as in Case b:

$$x_h = (R_i^2 - b^2)^{1/2} \qquad (3.2.26a)$$

$$y_h = b \qquad (3.2.26b)$$

Now the equation of line AB can be given by:

$$y = b + H \qquad (3.2.26c)$$

The point of inter section (T_i) of line AB and the ith failure circle can be given by(x_T, y_T).

Where,

$$y_T = b + H \qquad (3.2.26d)$$

$$x_T = \sqrt{R_i^2 - (b+h)^2} \qquad (3.2.26e)$$

Chord length:

$$T_i P_i = \sqrt{((x_h - x_T)^2 + (y_h - y_T)^2)}$$

Hence, $$\mathrm{Sin}^{-1}\left(\frac{H}{T_i P_i}\right) = \lambda_i \qquad (3.2.26f)$$

and $$\mathrm{Sin}^{-1}\left(\frac{T_i P_i}{2 R_i}\right) = \alpha_i \qquad (3.2.26g)$$

Driving and Resisting Moment:

Knowing all these values we can represent the expressions for driving moment of ith slice for both the two cases, i.e. Strength constant with depth and strength increasing with depth.

Case I: Constant Strength-

Driving moment,

$$M^o_{di} = \frac{H_i^3}{12}\left[1 - 2\,\mathrm{Cot}^2\rho + 3\,\mathrm{Cot}\lambda_i\,\mathrm{Cot}\beta + 3\,\mathrm{Cot}\,\alpha_i\,\mathrm{Cot}\lambda_i - 3\,\mathrm{Cot}\,\alpha_i\,\mathrm{Cot}\beta\right] dz_i \qquad (3.2.27)$$

Resisting moment,

$$M^o_{ri} = 2\,\alpha_i\,R_i^2\,c.ds_i \qquad (3.2.28)$$

Case II: Strength Increasing with Depth:

In this case also the expression for driving moment of ith slice can be given by equation (3.2.27). Resisting moment,

$$M^{o}_{ri} = \frac{k\, H_i^2\, ds_i}{4\, \mathrm{Sin}^2 \alpha_i\, \mathrm{Sin}^2 \lambda_i} \left[\mathrm{Cot}\lambda_i + \alpha_i (1 - \mathrm{Cot}\, \alpha_i\, \mathrm{Cot}\lambda_i) \right] \qquad (3.2.28)$$

Finally three-dimensional factor of safety can be given by:

$$F^{*} = \frac{M^{o}_{r} \cdot l_c + \sum_{i=1}^{n} M^{o}_{ri}}{M^{o}_{d} \cdot l_c + \sum_{i=1}^{n} M^{o}_{di}} \qquad (3.2.29)$$

where n is the total number of slice at the edge portion. Results obtained by using the computer programme(Appendix A) in terms of F^{*}/ F_{omin} will be presented in the following Chapters.

CHAPTER IV

PRESENTATION AND DISCUSSION OF RESULTS

4.1 Vertical Cut:

Results obtained from the analysis of vertical cut considering three types of failure surfaces namely, cylinder with planer edge surface, cylinder attached to a cone and cylinder attached to an ellipsoid are represented here in the form of dimensionless plots bringing out the effect of dimensions of edge portion in comparison with those of cylindrical part of the failure surface.

In case of conical edge shear surface attached to a cylinder, Fig. 4.1 shows the ratio F^*/F_{omin} as plotted against l/H for various values of l_c/H, for the two cases, i.e. strength constant with depth and strength increasing with depth. Here F^* represents the three-dimensional factor of safety, F_{omin} represents the least two-dimensional factor of safety. Figs. 4.2 and 4.3 represent the results for ellipsoidal edge surface, for the two cases, i.e., strength constant with depth and strength increasing with depth respectively. From these figures following observations may be made:

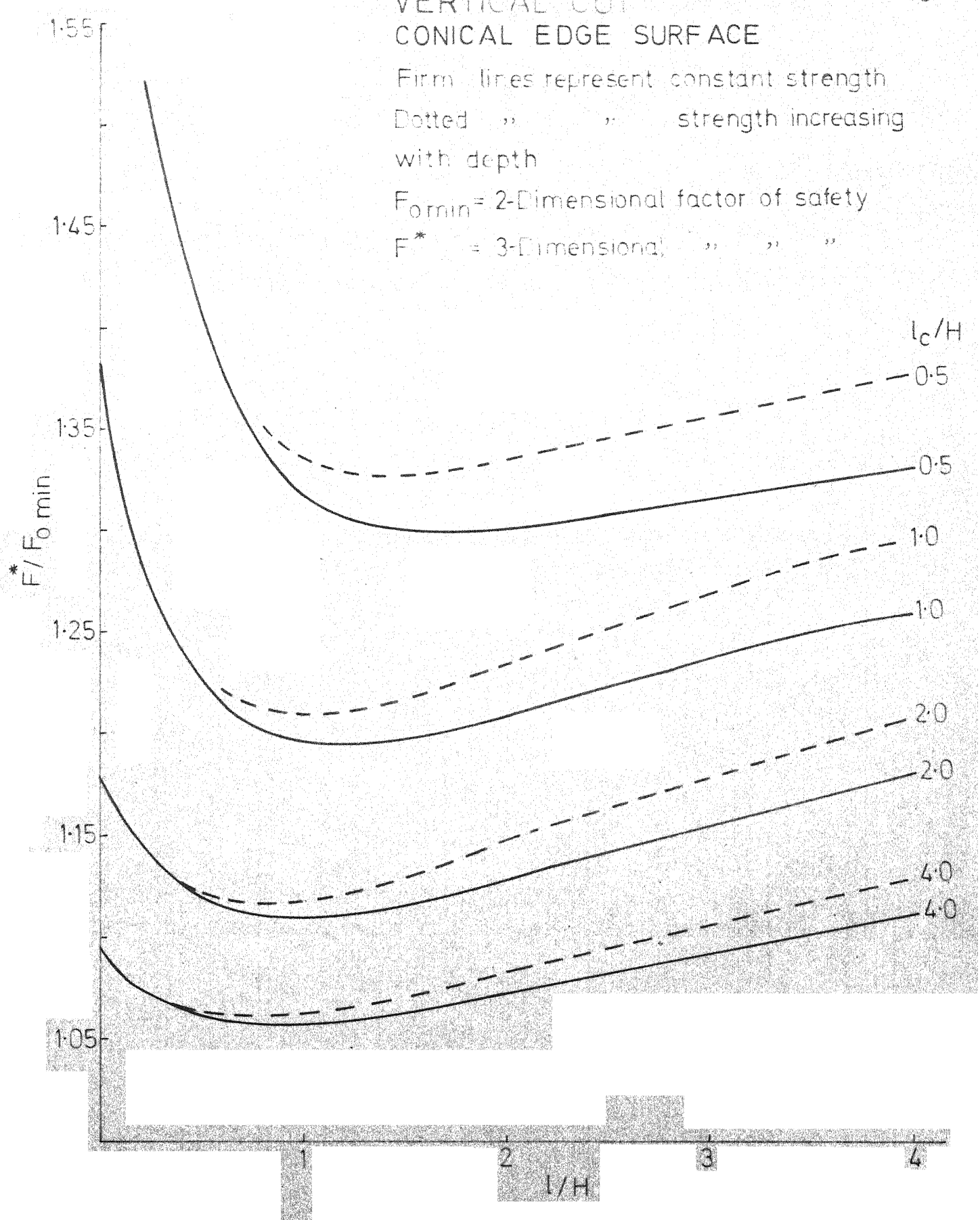

FIG 4·1 EFFECT OF SHEAR SURFACE GEOMETRY ON THE FACTOR OF SAFETY

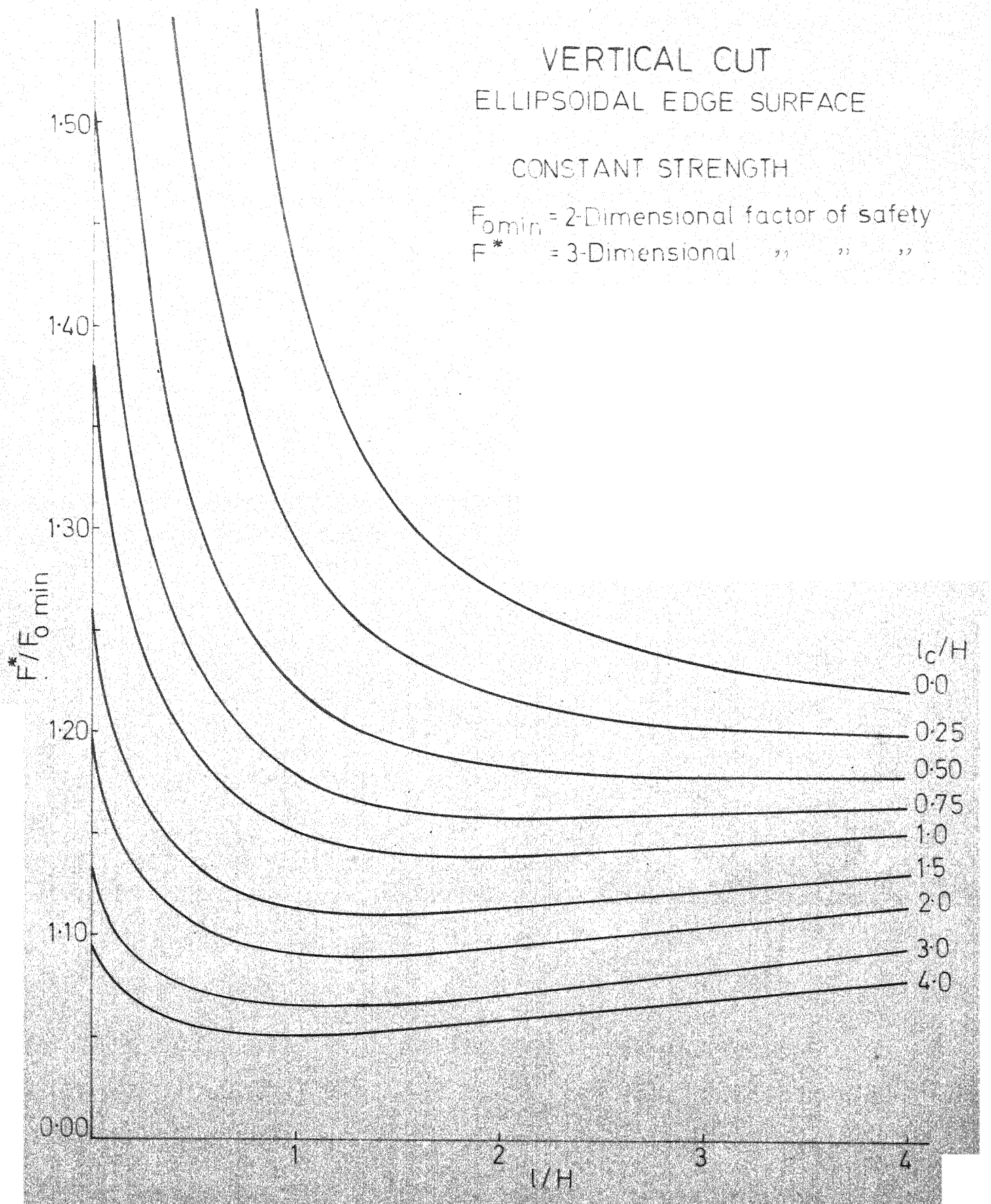

FIG.4·2 EFFECT OF SHEAR SURFACE GEOMETRY ON THE FACTOR OF SAFETY

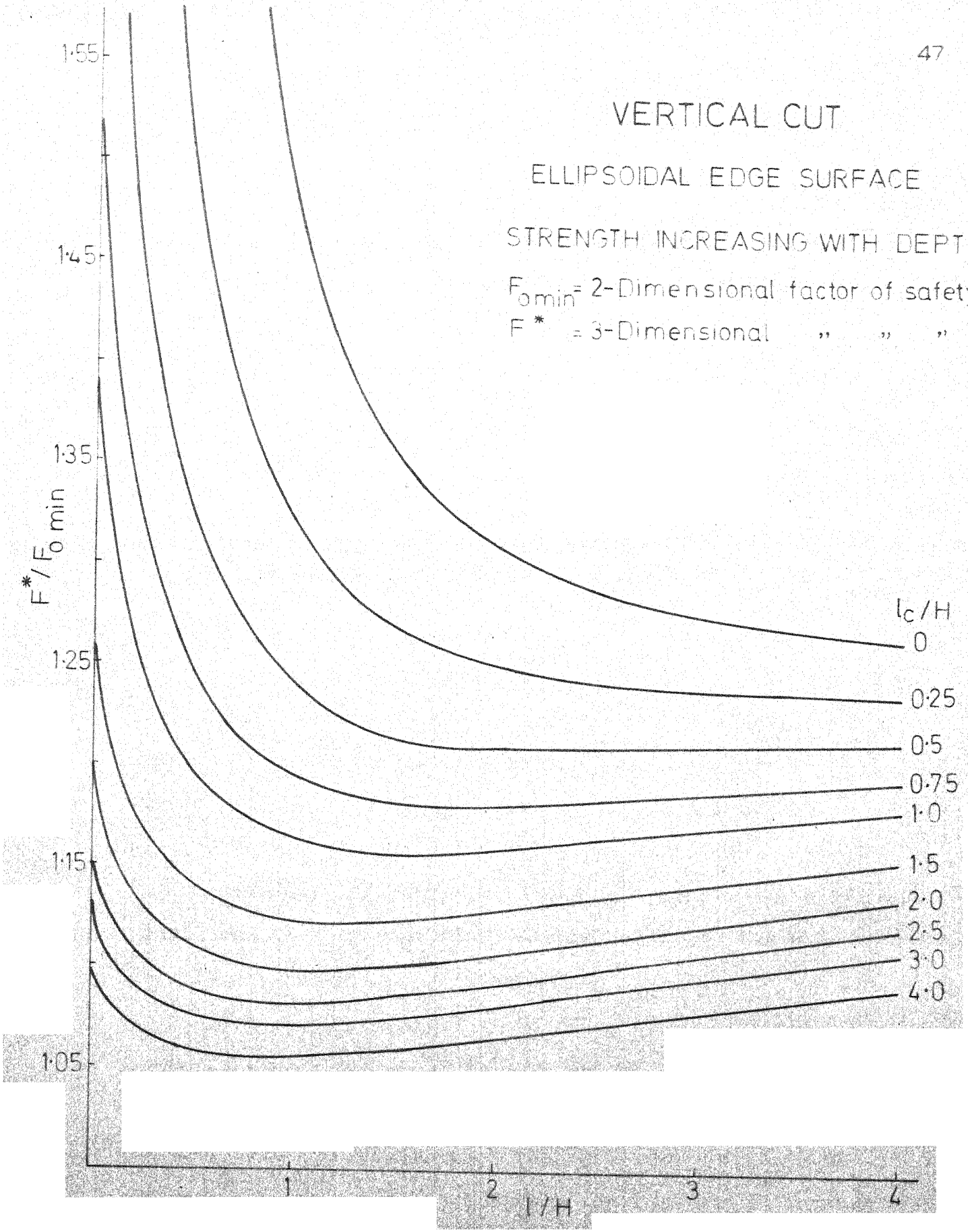

FIG. 4·3 EFFECT OF SHEAR SURFACE GEOMETRY ON THE FACTOR OF SAFETY

i) Since F^*/F_{omin} is always greater than unity, F^* always exceeds F_{omin}. For greater values of l_c/H, the ratio of F^*/F_{omin} becomes close to unity indicating that the edge portion has very little effect on the overall stability of the cut and the problem is simplified to plane-strain problem.

ii) The ratio F^*/F_{omin} is independent of the geometry of the cut and the strength of soil but F^* and F_{omin} individually depend on the geometry and the strength of soil.

iii) In case of cylinder with planer edge surface ($l/H = 0$) as the additional resiting moment is available from the planer edge with no alteration in the driving moment, the ratio F^*/F_{omin} becomes maximum for any value of l_c/H (Figs. 4.1 , 4.2 and 4.3).

iv) Failure surface having l_c/H greater than 4 can be considered to represent plane-strain condition for all practical purposes. For fixed values of l_c/H the F^* reaches a minimum at the critical value of l/H which determines the most likely length of failure surface.

v) It can also be seen that, for the problem of vertical cuts in purely cohesive homogenous soil, ellipsoidal failure surface gives consistantly lower values of F^* than for conical failure surface and is therefore lmost likely

to represent actual failure in the field. Similar conclusion has been arrived by Baligh and Azzouz (1976).

For predicting the 3-D factor of safety of vertical cut only ellipsoidal type failure surfaces are considered. From Figs. 4.2 and 4.3 it is seen that for an infinite vertical cut it is not possible to predict the actual length as the ratio of F^*/F_{omin} is continuously decreasing and approaches unity with the increasing values of l_c/H. In ideal case, the failure length should be infinite ($\frac{l_c}{H} = \infty$). But in practice failure may have a finite length due to non homogenuity of soil.

For a finite vertical cut also, it is not possible to predict F^* directly from Figs. 4.2 and 4.3 as there may be many combinations of l_c/H and l/H, and it is difficult to find which of these will give minimum F^*. A trial and error method is suggested to predict the value of F* for finite vertical cut.

If the total length of the cut is 2L then,

$$l_c/H + l/H = L/H \qquad (4.1)$$

Should always be satisfied for any combination of l_c/H and R/H. In a plot of l_c/H against l/H, equation (4.1) can be represented by a 45^o line cutting both l_c/H and l/H axes at a distance L/H from the origin (Fig.4.4 and 4.5)

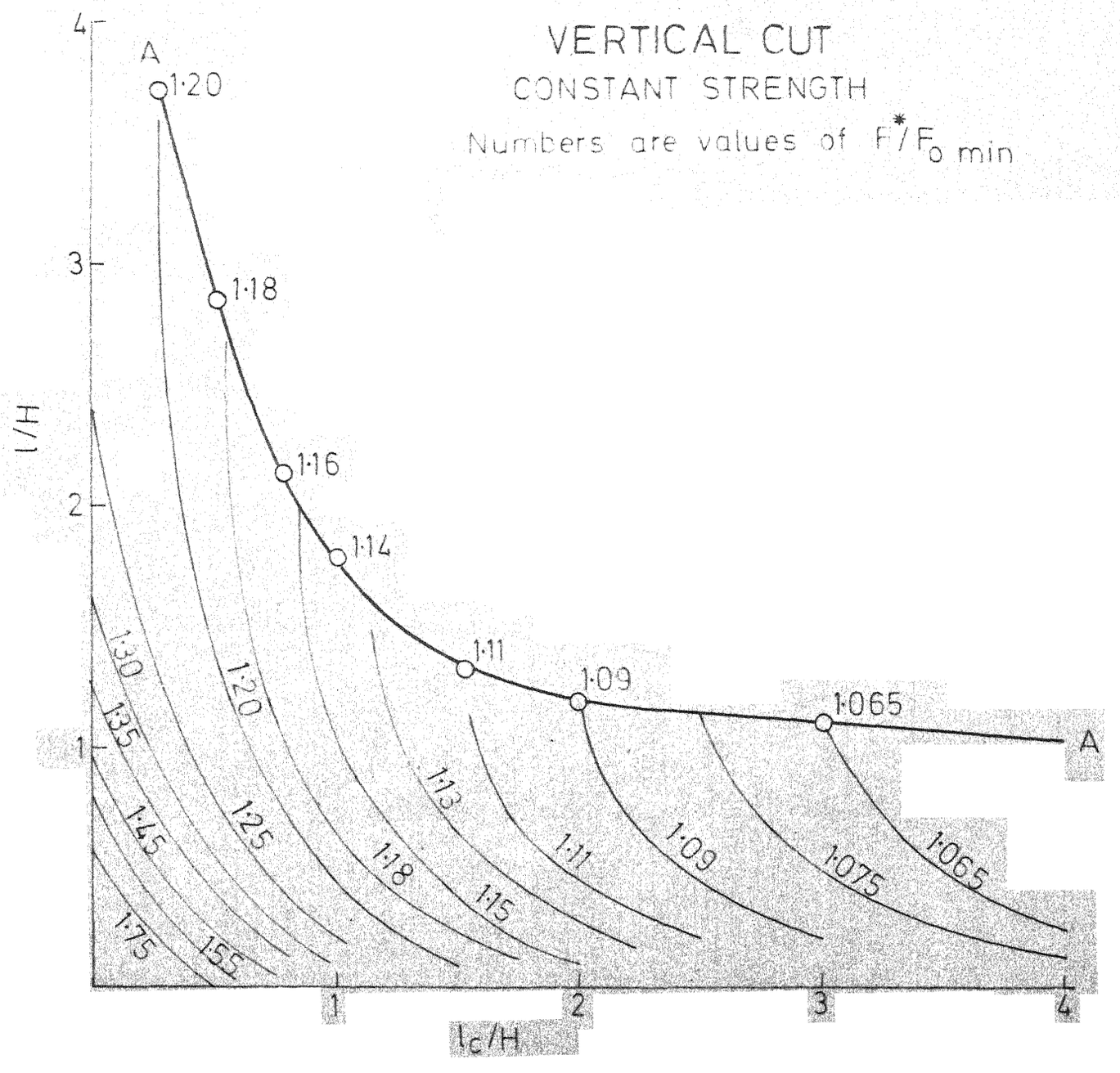

FIG·44 CONTOURS OF EQUAL $F^*/F_{o\,min}$

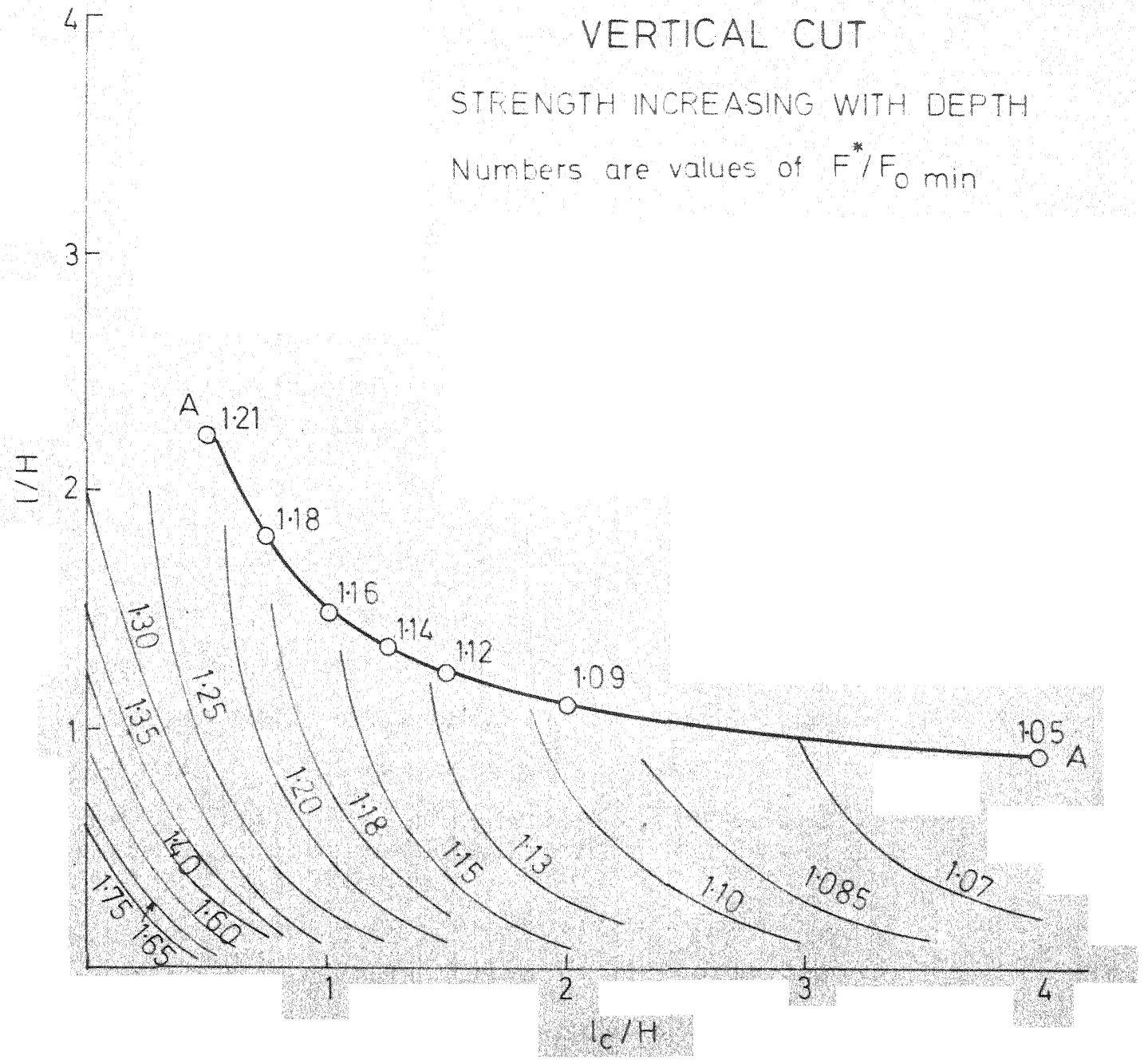

FIG·4·5 CONTOURS OF EQUAL $F^*/F_{o\,min}$

As both L and H are known, this line can easily be drawn in the plot of l_c/H against $1/H$. Every point on this line represents a probable combination of l_c/H and $1/H$ satisfying equation 4.1.

Contours of equal F^*/F_{omin} are also drawn in these plots. The shape of these curves for the two cases, viz., constant strength and strength increasing with depth, are represented in Figs. 4.4 and 4.5 respectively. These curves are concave upwards and with increasing values of F^*/F_{omin} the curves shift downwords.

Contour of minimum F^*/F_{omin} has also been drawn, above which no combination of l_c/H and $1/H$ is possible. From these figures it is obvious that, the contour of F^*/F_{omin} which is tangent to the line represented by equation 4.1 will represent the critical value of F^*/F_{omin} for the finite vertical cut having total length 2L. For a given 45^o straight line the appropriate contour of F^*/F_{omin}, which is tangent to this line, can be interpolated with the help of Figs. 4.2 or 4.3 for the two cases of the strengths of the soil. The point of tangency will give the critical values of $1/H$ and l_c/H.

Fig. 4.6 gives values of F^*/F_{omin} for a value of $L/H = 1.83$ using the following shapes of edge surfaces:

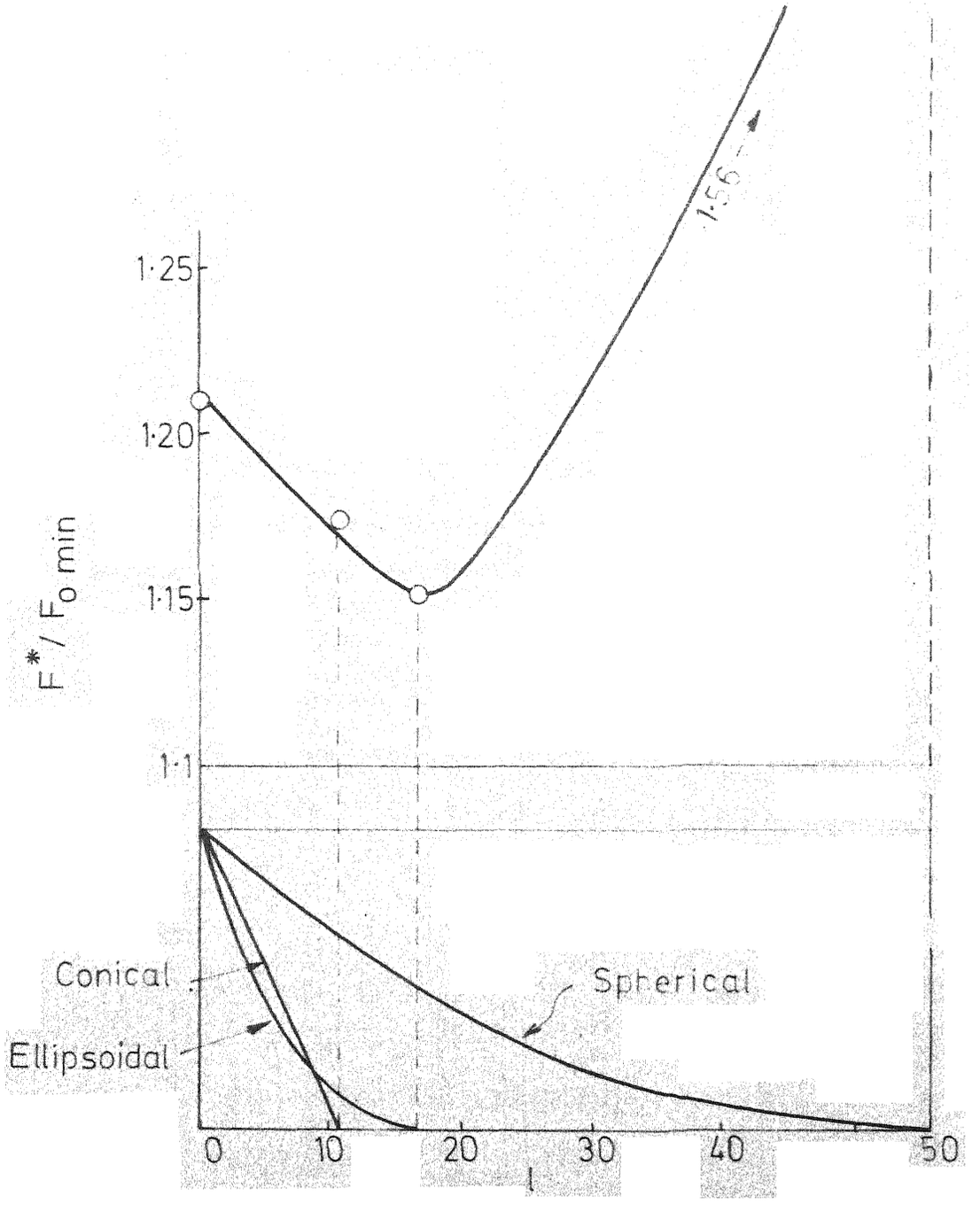

FIG. 4·6 VARIATION OF $F^*/F_{o\,min}$ WITH DIFFERENT EDGE SURFACES

1) Cylinder with planer edge.

2) Cylinder with conical edge surface

3) Cylinder with ellipsoidal edge surface and

4) Cylinder with spherical edge surface.

It will be seen that the ellipsoidal edge surface gives the minimum value of F^*/F_{omin}. All the surfaces considered are either linear or convex. Even though one would have expected conical surface to give the least value but due to different values of l/H and l_c/H in case of conical and ellipsoidal surfaces, the relationship between driving and resisting moments gives a smaller value of F^*/F_{omin} for ellipsoidal edge surface. This figure suggests that of the four surfaces considered, ellipsoidal edge surface, for the mechanism adopted here, gives the lowest value of F^*/F_{omin}.

4.2 Slopes:

In the case of slopes the 3-D factor of safety(F^*) will also depend on the slope angle β . To make a comparison, how the slope angle β effects the 3-D factor of safety(F^*) with that obtained for a vertical cut, a homogeneous clay slope with $\beta = 10^o$, 30^o, 45^o, and 60^o are thoroughly analysed for ellipsoidal edge surfaces only.

For the 10^{o} slope also, F^{*}/F_{omin} is plotted against l/H for different values of l_c/H for two cases i.e. constant strength and strength increasing with depth (Fig.4.7 and 4.8). From these figures contours of equal factor of safety are also drawn for the above mentioned cases (Fig.4.9 and 4.10). The nature of these curves are same as they were in case of vertical cuts.

Using Figs.4.9 and 4.10 $L/\Delta R$ is plotted against F^{*}/F_{omin}. Figs. 4.11 and 4.12 show these relationships for the two cases respectively

where, $\Delta R = R_{max} - u$ (Figs. 4.11 and 4.12) and R_{max} is the radius of circle obtained from 2-D analysis. Results for a vertical cut are also indicated in Figs. 4.11 and 4.12. The curves $L/\Delta R$ vs F^{*}/F_{omin} for all the intermediate slope angle will be within the narrow band provided by $\beta = 10^{o}$ and $\beta = 90^{o}$. From these figures it can be concluded that, slope angle has a little influence on the ratio F^{*}/F_{omin} above certain values of $L/\Delta R$.

As for example, from Fig. 4.11 and 4.12 it is seen that the difference in the ratio of $\frac{F^{*}}{F_{omin}}$ for $\beta = 10^{o}$ and $\beta = 90^{o}$ for $L/\Delta R = 1.5$ is approximately 2% and this small difference can be neglected. So for the slopes having

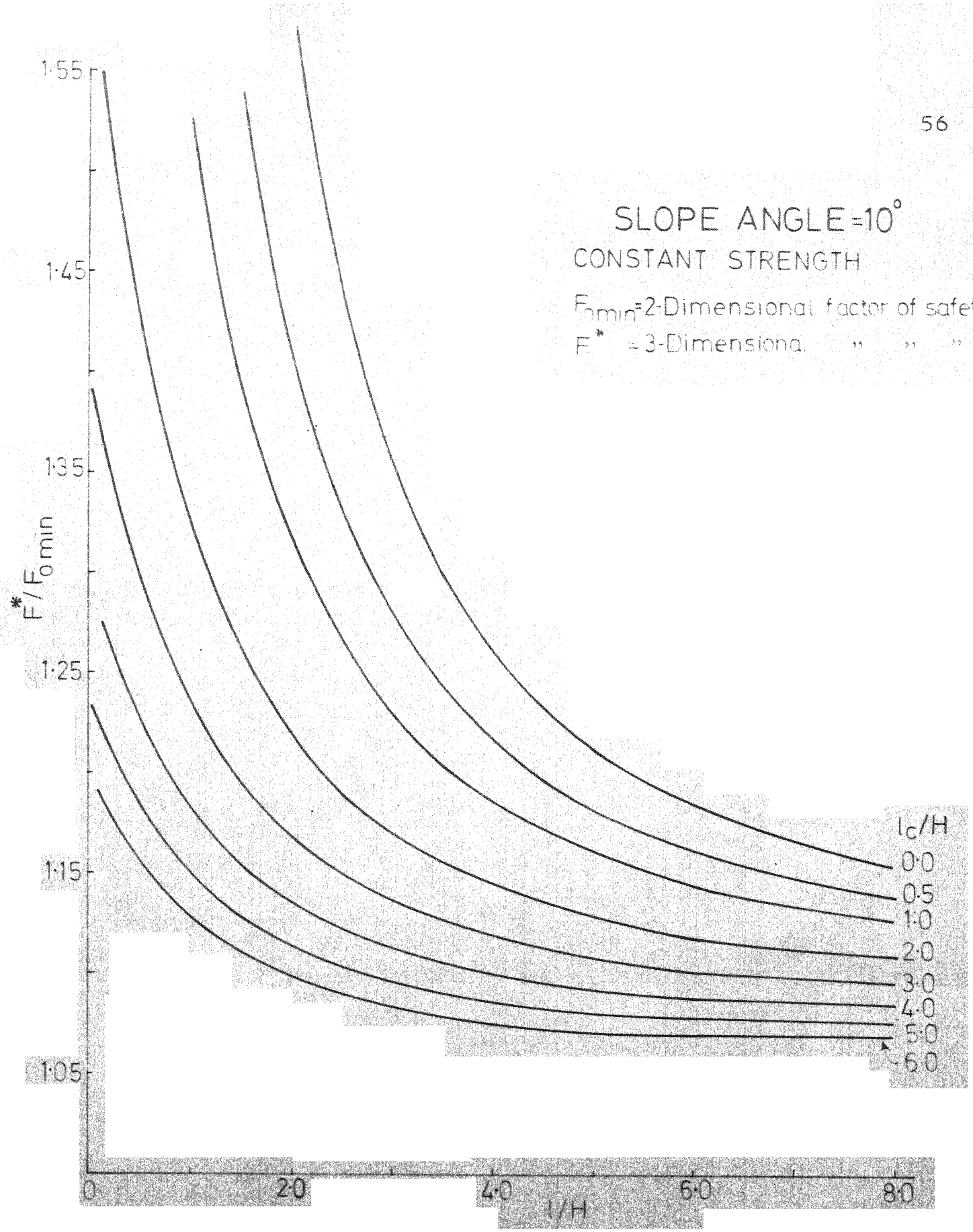

FIG. 4·7 EFFECT OF SHEAR SURFACE GEOMETRY ON THE FACTOR OF SAFETY

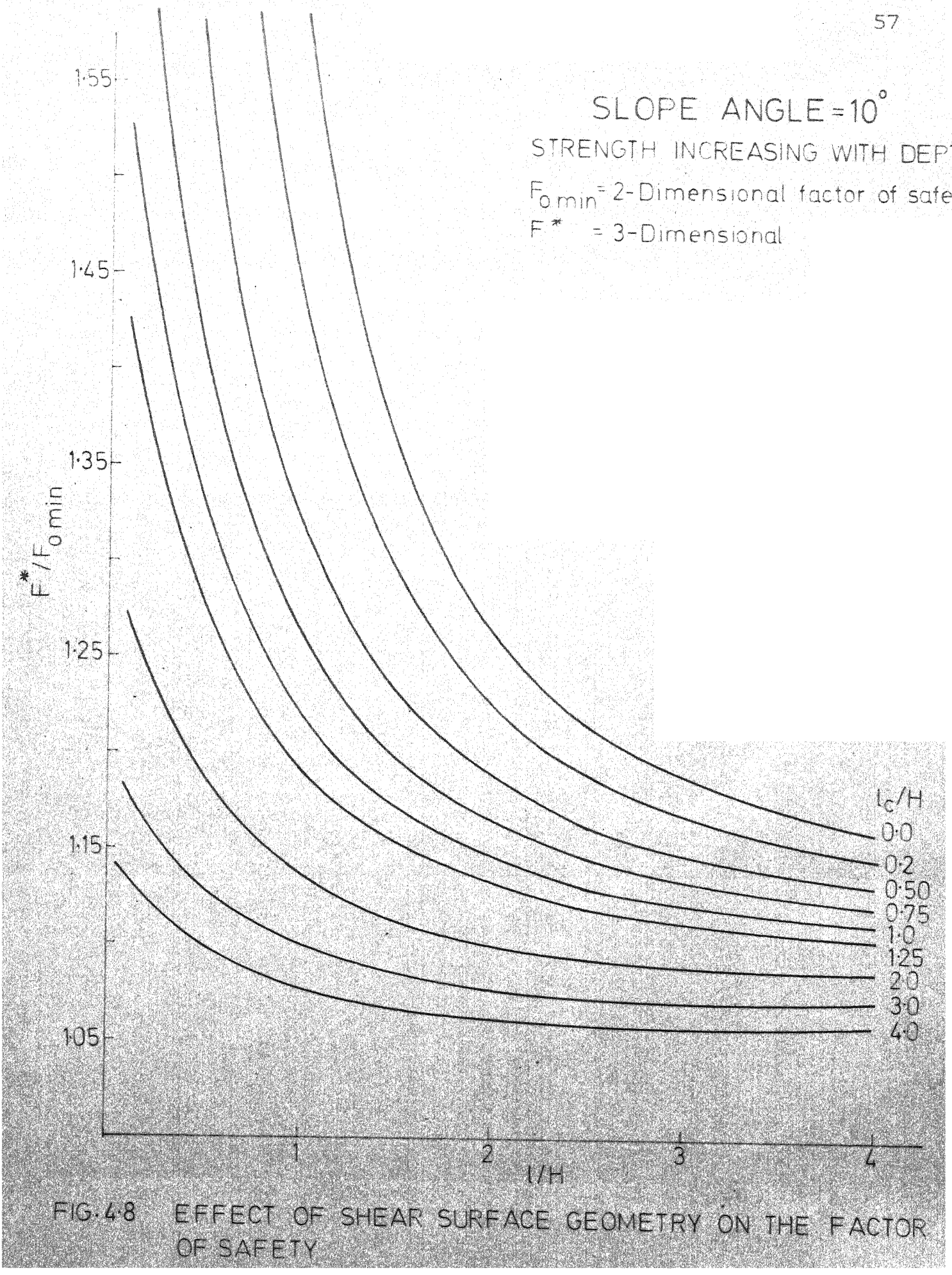

FIG. 4·8 EFFECT OF SHEAR SURFACE GEOMETRY ON THE FACTOR OF SAFETY

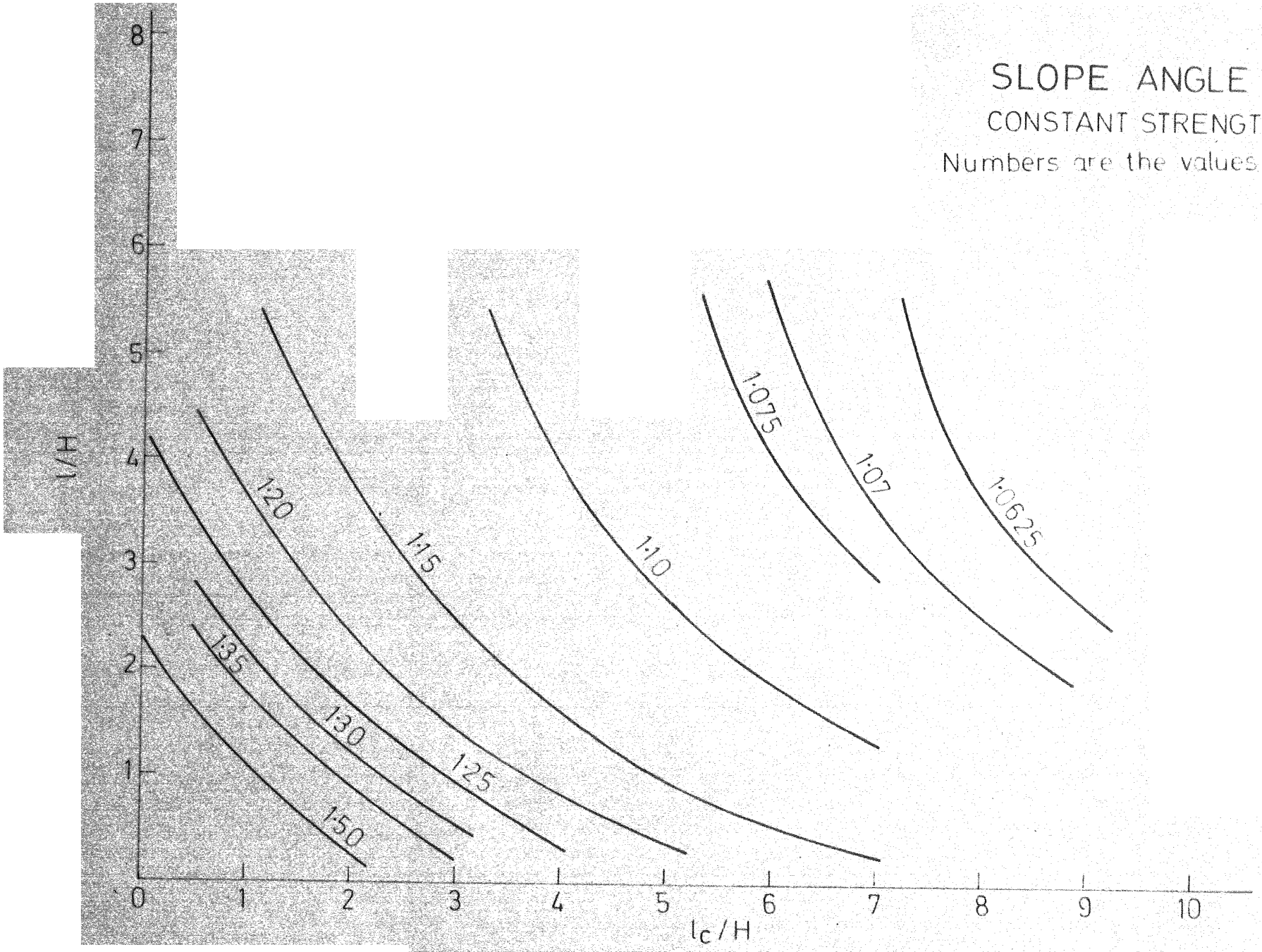

FIG 4·9 CONTOURS OF EQUAL $F^*/F_{o\,min}$

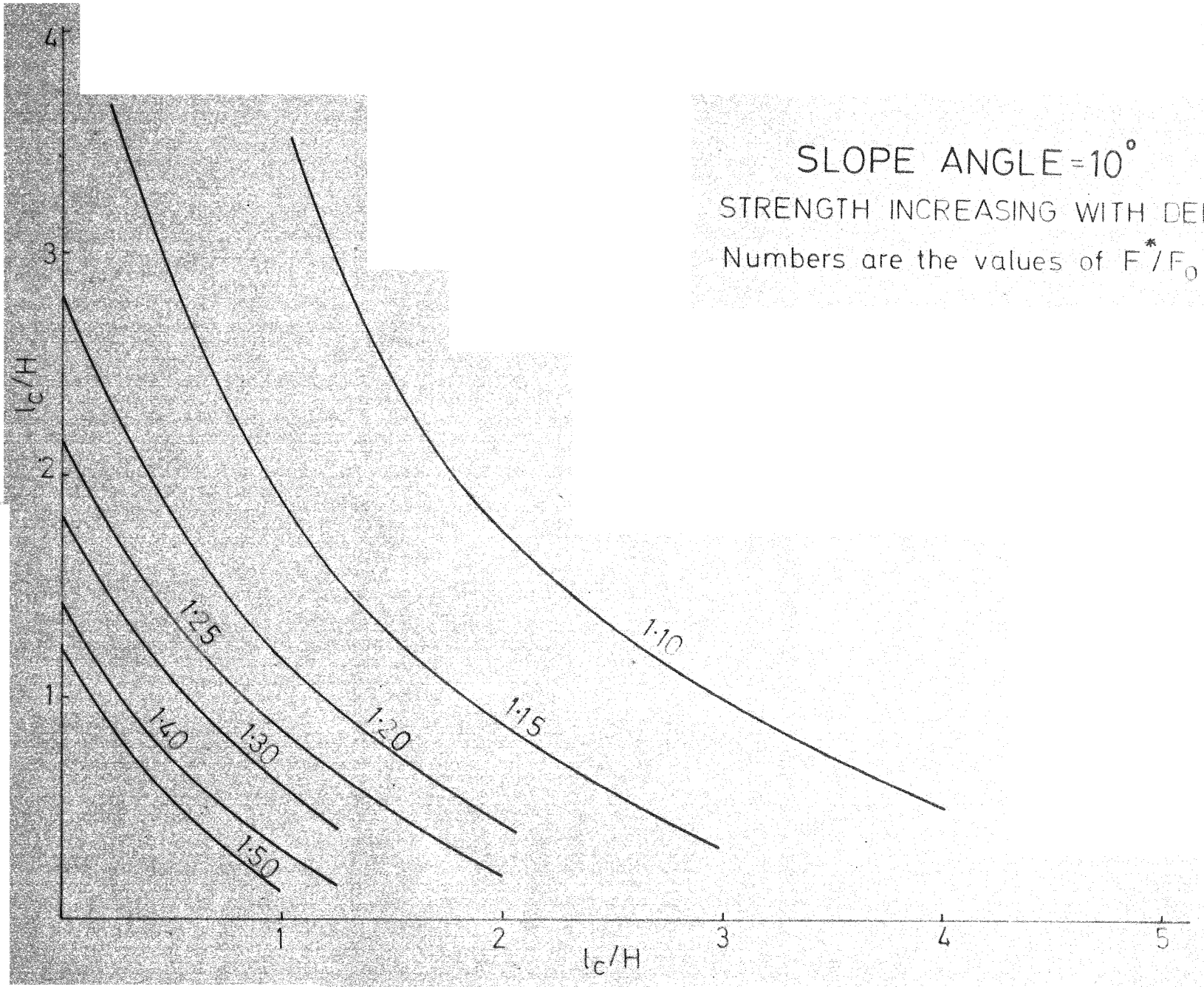

FIG·4·10 CONTOURS OF EQUAL $F^*/F_{0\,min}$

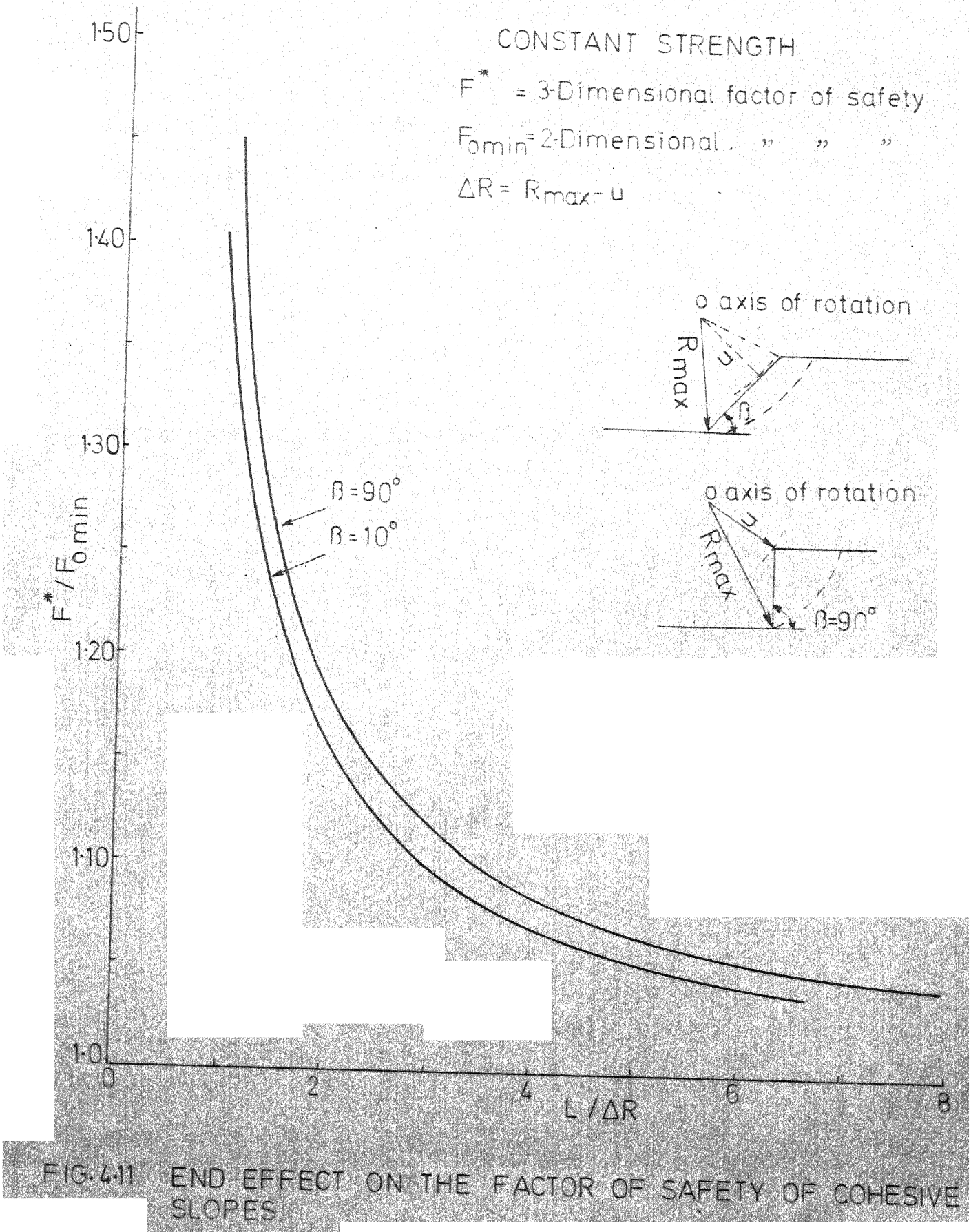

FIG. 4.11 END EFFECT ON THE FACTOR OF SAFETY OF COHESIVE SLOPES

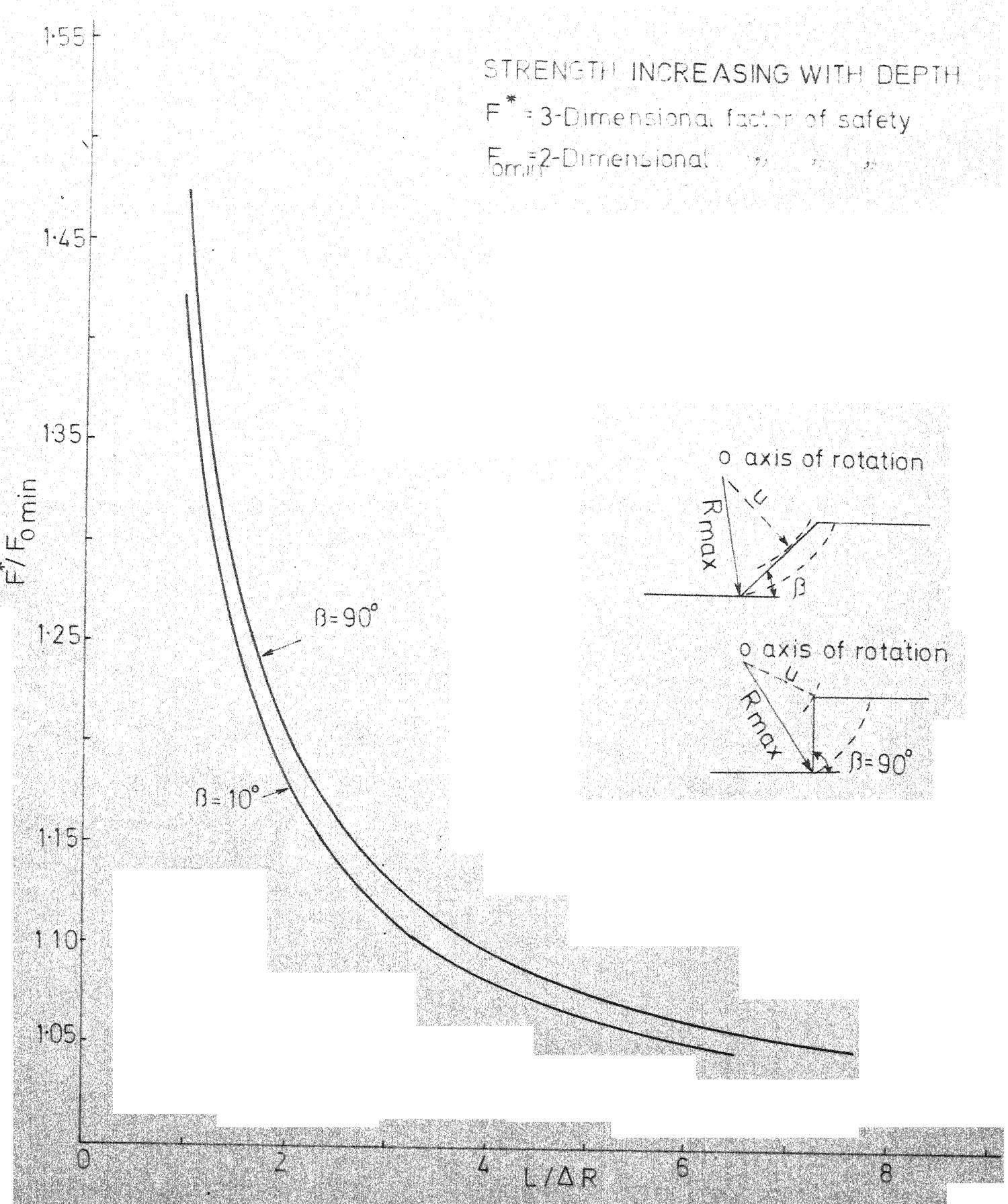

FIG·4·12 END EFFECT ON THE FACTOR OF SAFETY OF COHESIVE SLOPES

l/ $\Delta R > 1.5$, F^*/F_{omin} value can be taken corresponding to $\beta = 90^\circ$.

In Figs. 4.13 and 4.14 contours of equal F^*/F_{omin} have been drawn in plots of l/H against the slope angle(β) for the two cases, namely, (1) Constant strength, (2) Strength increasing with depth respectively. From these Figures it can be seen that for same values of F^*/F_{omin}, the length of the edge portion is increasing with the decreasing values of slope angle (β). However within the range of slope angle (β) from 45° to 90°, this change in the ratio of l/H is not significant but for the values of β less than 45° the change in the ratio of l/H is much more.

Obtaining the F^*/F_{omin} from Figs. 4.11 or 4.12 one can enter in Fig. 4.13 or 4.14 respectively to get the value of l/H for a particular slope angle (β). Figs.4.15 and 4.16 represent the view of the failure surface on a plane along which the maximum depth of failure occur, for two cases, strength constant with depth and strength increasing with depth. These figures are drawn for a 6 meter deep cut with slope angle varies from 10° to 90° and the total length of the cut is assumed as 18 meter. For example, with $\beta = 60^\circ$, the value of R is found as 4.5 meter for the case when strength is constant with

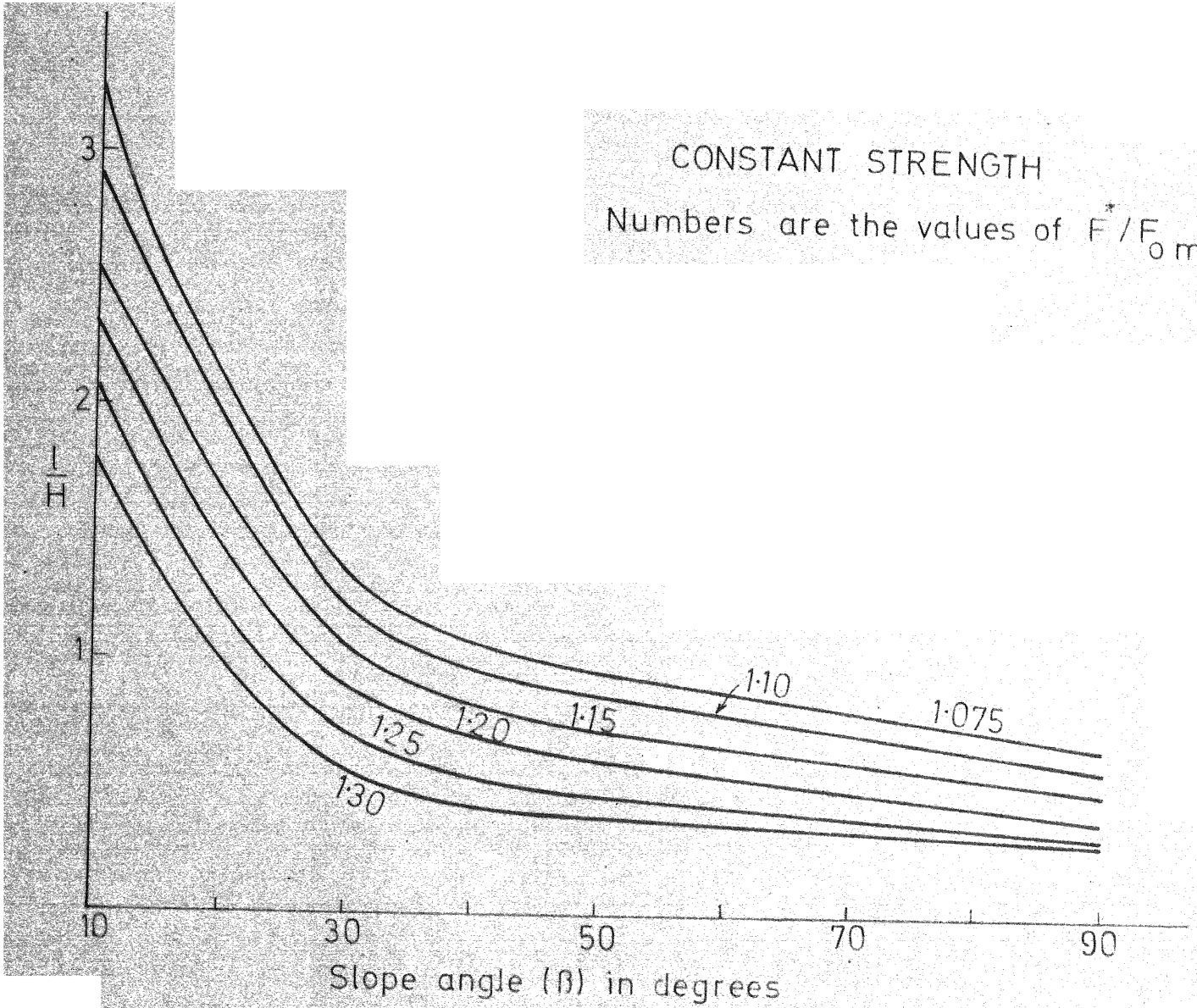

FIG. 4.13 EDGE EFFECTS AS FUNCTION OF SLOPE ANGLE

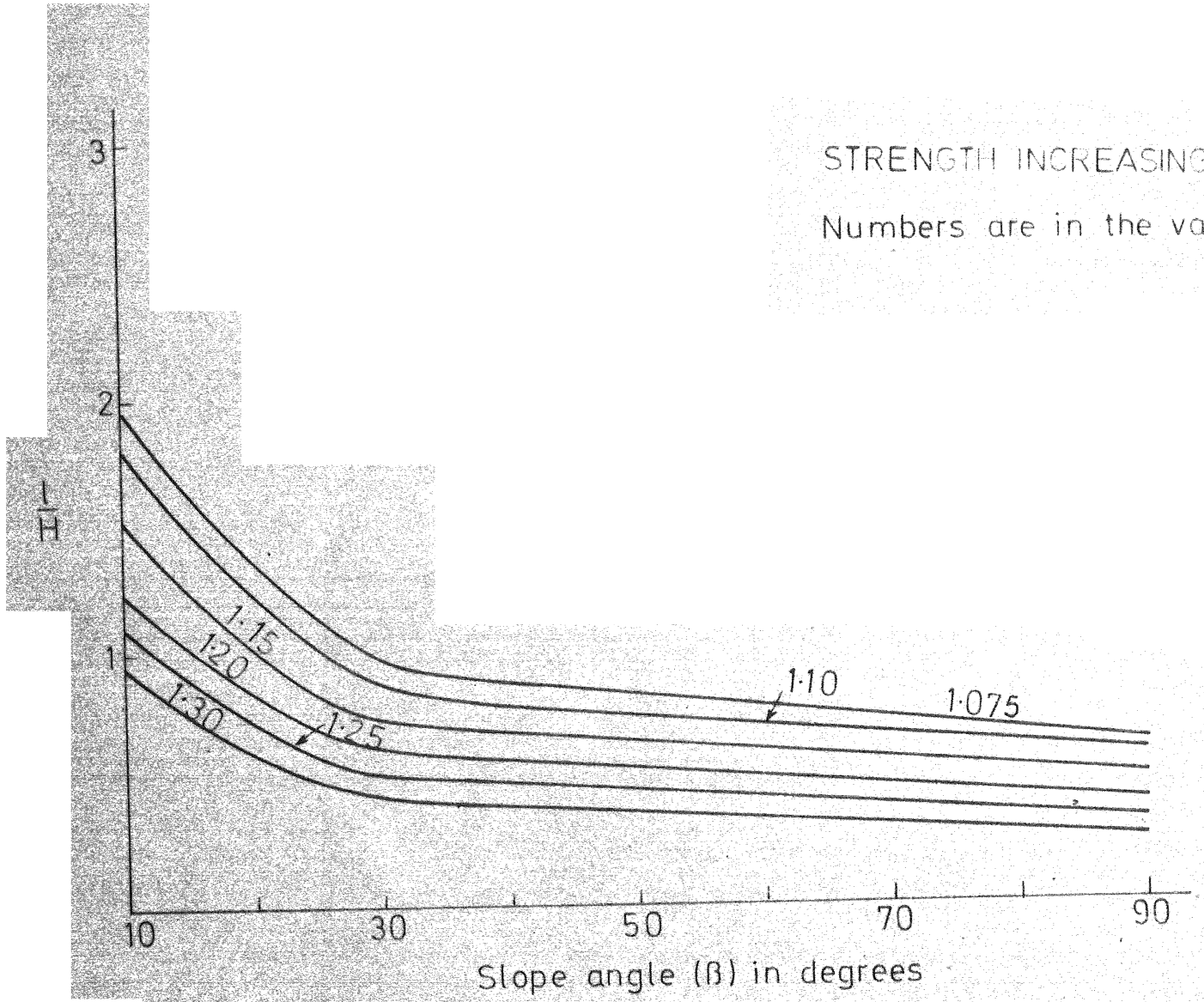

FIG. 4·14 EDGE EFFECTS AS FUNCTION OF SLOPE ANGLE

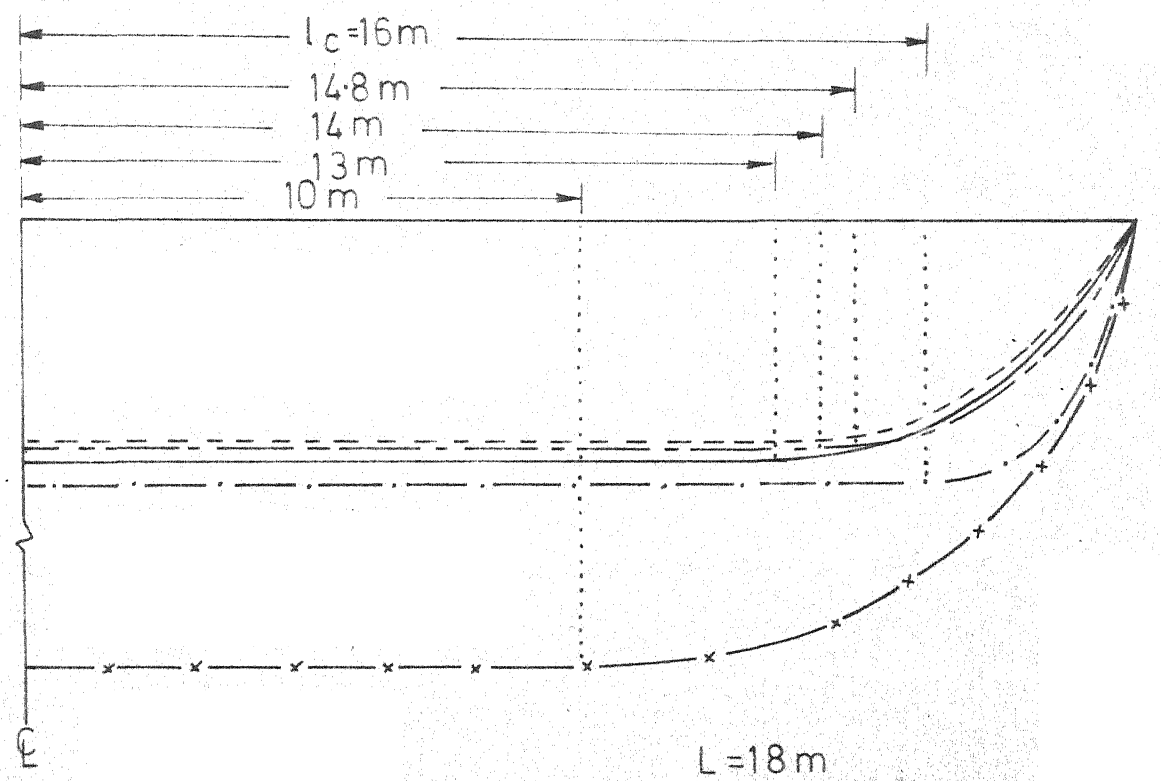

FIG. 4.16 VARIATION OF THE SHAPE OF THE FAILURE SURFACE WITH SLOPE ANGLE

depth. The value of $L/\Delta R$ is found as 4.05, and from Fig. 4.11 the corresponding F^*/F_{omin} is found as 1.075. With this value of F^*/F_{omin} and $\beta = 60^\circ$, the value of l/H is found as 0.9 from Fig. 4.13. So the length of the edge portion should be 5.4 meter to achieve $F^*/F_{omin} = 1.075$.

Similar procedure has been adopted for the second case also, i.e. when strength is increasing with depth. Figs. 14.15 and 14.16 bring out a very significant aspect of slope failures in cohesive homogeneous clays. It will be seen that for flat slopes, $\beta \approx 10^\circ$, the shape of the failure surface is markedly controlled by the edge portions ($\frac{l}{l_c} = 1.5$ and 1.0 for two cases respectively). Such an observation has been reported from the study of mud flows on flat slopes by Bhandari, (1970).

As the slope angle increases beyond 45° degrees the edge effects are about the same upto $\beta = 90^\circ$.

CHAPTER - V

CONCLUSIONS & RECOMMENDATIONS

Based on the study of effects of shapes of edge surfaces in homogenous cohesive clay with strength constant with depth and increasing with depth, the following main conclusions are derived.

1. For a given cut the 3-D stability, F^*/F_{omin} is shown to be controlled by the shape of edge surfaces, length of cylindrical and edge portions. (Figs. 4.1, 4.2 and 4.3).

2. The ellipsoidal edge surface is shown to be the most critical one and it is suggested that it may represent the field situation (Fig . 4.6).

3. Contours of equal F^*/F_{omin} (Figs. 4.4 and 4.5) are presented and it is shown that all the limiting cases lie within the relationship indicated by the line AA. It is also seen that in homogeneous material the full length of the cut will give the minimum value of the ratio F^*/F_{omin}.

4. Using the contours of F^*/F_{omin} a trial and error method has been suggested to evaluate F^*/F_{omin} for a finite cut. This is very important to practicing engineers in the determination of additional stability of cuts and slopes due to edge effects.

5. The effects of slope angle on the value of F^*/F_{omin} has been brought out (Fig. 4.13 and 4.14) It is shown that the contribution to stability from edge effects is very large for shallow slopes and the contribution decreases as the slope angle increases. The significance of this conclusion for flat slopes is very relavant to the study of mud flows on gentle slope. The amount of mass involved in failure is also shown to depend on the slope angle.

As this study was aimed at evaluating the effect of various parameters on contribution of edge effects to stability of cuts and slopes a rigid body mechanism assuming the same linear axis of rotation was considered. It is felt

that now it is important to consider a more realistic mechanism in which the edge portions and the cylindrical part are taken to rotate about different centres of rotation. Such a study is expected to refine the details presented in this thesis, however overall conclusion arrived at are not likely to change significantly.

The other important line of investigation in this respect would be an effective stress analysis.

REFERENCES

1. Baligh, M.M., and Azzouz,S., 1975, "End Effects on the Stability of Cohesive Slopes", Proc. ASCE Journal of the Geotechnical Engineering Division, Vol.101.

2. Bhandari, R.K.,1970,"Mudflows in Stiff Fissured Clays", Ph.D. Thesis, Empirical College, University of London.

3. Bjerrum,L., 1973, "Problems on Soil Mechanics and Construction on Soft Clays", Norwegian Geothechnical Institute, 100.

4. Gibson, R.E., and Morgenstern, N.,1962," A Note on the Stability of Cuttings in Normally Consolidated Clays", Geotechnique, Vol.12.

5. Lambe, T.W., and Whitman, R.V., 1969, "Soil Mechanics", Wiley Publication.

6. Sherard, J.L., et.al., 1963, "Earth and Earth-Rock Dams", Wiley publication.

7. Taylor, D.W., 1937, "Stability of Earth Slopes", Journal of the Boston Society of Civil Engineers.

8. Yudhbir and Varadarajan, A., 1975, "Influence of Shear Zones on the Mechanism of Stability of the Foundation of Beas Dam, India. Eng. Geol.,9:53-62.

ADDITIONAL REFERENCES

1. Bishop, A.W., 1955, "The Use of Slip Circle in the Stability Analysis of Earth Slopes", Geotechnique, Vol.5.

2. Morgenstern, N.R. and Price, V.E., 1965, "The Analysis of Stability of General Slip Surfaces", Geotechnique, Vol.15.

3. Spencer, E., 1967, "A Method of Analysis of the Stability of Embankments Assuming Parallel Interslice Forces", Geotechnique. XVII No.-1, pp. 11-26.

4. Whitman, R.V. and Bailey, W.A., 1967, "Use of Computers for Slope Stability Analysis," Proc. ASCE, Vol.93, No. SM4.

APPENDIX

```
C
C
C           TWO DIMENSIONAL FACTOR OF SAFETY
C
C           SEARCHING FOR CRITICAL CIRCLE
C
      COMMON/LEV1/ H,SHY,RAD2,A2,B2, SL,DM2,RM2,MC,MR,LC,GUM
      REAL  MC,MR,LC
C
 10   FORMAT(3F6.2,F5.2)
 11   FORMAT( I1)
 2020 FORMAT(//10X,*RADIUS OF THE CRITICAL CIRCLE =*,E15.8/10X,
     1*MINIMUM FACTOR OF SAFETY =*,F10.7/10X,*ETA =*,F6.2/10X,
     2*DRIVING MOMENT =*,F20.8/10X,*RESISTING MOMENT =*,F20.8)
 2010 FORMAT(//10X,*A = *,E15.8)
 1002 FORMAT(//10X,*PLANNER RESISTING MOMENT = *,E15.8)
 1030 FORMAT(//12X,*D*,8X,*B*,10X,*FS*,12X,*FS/FC*,8X,*L/DELR*/
     110X,80(1H=))
 1111 FORMAT(/10X,*R (MIN) = *,F12.5)
 1040 FORMAT(10X,F5.2,5X,F5.2,5X,F10.6,5X,F10.6,5X,F9.4,5X,I3,5X,
     1E15.8,5X,E15.8)
 3010 FORMAT(/10X,F20.8,10X,F15.8,10X,F20.8,10X,E15.8)
 1010 FORMAT(/10X,F9.4,5X,F20.8,6X,F20.8,6X,F10.7,10X,E15.8)
 1020 FORMAT(//12X,*R*,12X,*MRC*,24X,*MDC*,20X,*FC*,18X,*RAD*)
 1060 FORMAT(//10X,*DRIVING MOMENT(CRITICAL) = *,F20.8/
     110X,*RESISTING MOMENT(CRITICAL) = *,F20.8)
 1070 FORMAT(/10X,80(1H-))
 2040 FORMAT(//10X,*SLOPE ANGLE = *,F7.3/10X,20(1H*))
 1080 FORMAT(//10X,*LAMDA = *,E15.8//10X,*A = *,F15.8//10X,*B = *,F15.8)
 1090 FORMAT(//10X,*FINAL RESULTS(FOR CRITICAL CIRCLE)*/10X,34(1H-))
 2030 FORMAT(/10X,100(1H*))
 2050 FORMAT(/10X,*THETA(DEGREES) = *,E15.8)
C     **********************************************************************
C
      READ(5,10) SU,GAMA,H,SHI
      WRITE(6,2040) SHI
C     READ IN THE TYPE OF SOIL
C     INDEX = 1, CONSTANT STRENGTH
C     INDEX = 2, STRENGTH INCREASING WITH DEPTH
      READ(5,11) INDEX
      IF(INDEX .EQ. 2)  CONST=SU
      FR=50.00
      EPS=0.0
      PAI=3.14159265
      SHY=SHI*PAI/180.
      KK=0
      LL=0
      ETA=35.0
      DO 2000 MN=1,200
      L=0
      K=0
      R=0.0
```

```
      FI=5C.CC
      CC 2CC N=1,2CC
      PHEE=ETA*PAI/18C.
      A=R*CCS(PHEE)
      B=R*SIN(PHEE)
      RAC=SQRT((H/SIN(SHY))**2+2.*H*(E-A*CCTAN(SHY))+R**2)
      X=ARCCS(B/RAD)
      EC=RAC*SIN(X)-A
      AB=SQRT((H/SIN(SHY))**2+2.*EC*H*CCTAN(SHY)+EC**2)
      THETA=ARSIN(AB/(2.*RAC))
      V=ARSIN(H/AB)
      VC=V*18C./PAI
      DMC=GAMA*(H**3)*(1.-2.*(CCTAN(SHY))**2+3.*CCTAN(SHY)*CCTAN(V)
     1-3.*CCTAN(SHY)*CCTAN(THETA)+3.*CCTAN(V)*CCTAN(THETA))/12.
      IF(INDEX .EQ. 2) GC TC 1CC
      RMC=2.*(RAD**2)*THETA*SL
      FC=RMC/DMC
      GC TC 1C1
1CC   RMC=CCNST*H*RAD*(CCTAN(V)+THETA*(1.-CCTAN(V)*CCTAN(THETA)))/
     1(2.*SIN(THETA)*SIN(V))
      FC=(CCTAN(V)+THETA*(1.-CCTAN(V)*CCTAN(THETA)))*GAMA*(H**3)/
     1(((SIN(THETA)*SIN(V))**2)*DMC*4.)
1C1   F=FC-FI
      IF(F .GT. C.0)GC TC 8CC
      FI=FC
      VC1=VC
      A1=A
      B1=B
      RAC1=RAC
      DM1=DMC
      RM1=RMC
      THETA2=THETA*18C./PAI
      IF(K .GT. C)GC TC 930
      R1=R
      R=R+1C.CC
      GC TC 2CC
8CC   K=K+1
930   CCNTINUE
      IF(L .GT. C)GC TC 9CC
      R=R1-1C.CC
      FI=5C.CC
9CC   CCNTINUE
      R=R+C.5
      L=1
      IF(K .GT. 1)GC TC 950
2CC   CONTINUE
950   R1=R-1.C
      FF=FI-FR
      IF(FF .GT. C.0)GC TO 8C0
      FR=FI
      R2=R1
      RAC2=RAD1
```

```
      DM2=DM1
      RM2=RM1
      VC2=VC1
      A2=A1
      B2=B1
      THETA3=THETA2
      IF(KK .GT. 0)GO TO 865
      ETA1=ETA
      ETA=ETA+5.00
      GO TO 2000
  860 KK=KK+1
  865 CONTINUE
      IF(LL .GT. 0)GO TO 880
      ETA=ETA1-5.00
      FR=50.00
  880 CONTINUE
      ETA=ETA+1.0
      LL=1
      IF(KK .GT. 1)GO TO 960
 2000 CONTINUE
  960 ETA1=ETA-2.00
C
      FI2=FR
      WRITE(6,1090)
      WRITE(6,2020) RAD2,FI2,ETA1,DM2,RM2
      WRITE(6,1080) VC2,A2,B2
      WRITE(6,2050) THETA3
      WRITE(6,2010) FR
      WRITE(6,2030)
C
C
C
C                  THREE DIMENSIONAL FACTOR OF SAFETY
C
C
C
C     READ IN THE TYPE OF EDGE SURFACE
C     ICNT =1, CONICAL EDGE
C     ICNT =2, ELLIPSOIDAL EDGE
      READ(5,11) ICNT
C     D IS THE RATIO LO/H
      D=0.0
      THETAO=THETA3*PAI/180.
      ETAO=ETA1*PAI/180.
      CALL EGREST
      WRITE(6,1002) GLN
      NK=0
      NNN=1
      GO TO 4
  805 IF(D .GE. 0.49)GO TO 3
      D=D+0.1
      GO TO 4
```

```
  3     IF(E .GE. 1.99)GO TO 33
        E=E+0.25
        GO TO 34
  33    E=E+0.5
  34    E=E+0.1
  4     CONTINUE
        LC=E*H
        IF(NK .GT. 0) WRITE(6,1070)
        CONTINUE
C       E IS THE RATIO L/H
        E=0.0
        IF(E .EQ. 0.0)GO TO 820
  810   IF(E .GE. 3.98)GO TO 816
        IF(E .GE. 0.49)GO TO 815
        E=E+0.1
C       DZ IS THE THICKNESS OF EACH SLICE
        DZ=0.05
        GO TO 830
  815   E=E+0.5
        DZ=0.25
        GO TO 830
  816   DZ=0.5
        E=E+0.5
        GO TO 830
  820   CONTINUE
        SUM=0.0
        TUM=0.0
        NCYCLE=0
C       DM2 AND RM2 ARE THE DRIVING AND RESISTING MOMENTS RESPECTIVELY
C       OBTAINED FROM 2-D ANALYSIS.
        MR=GUM+LC*RM2
        MD=LC*DM2
        GO TO 850
  830   CONTINUE
C       AL IS THE LENGTH OF EDGE PORTION
        AL=E*H
        AINDEX=SHI+ETA1
        AIND=AINDEX*PAI/180.
        IF(AINDEX .GE. 90.00)GO TO 835
        CS=R2*SIN(AIND)
        SC=R2*COS(AIND)
        IF(ICNT .EQ. 2) GO TO 12
        CL=RAD2*AL/(RAD2-CS)
        GO TO 840
  12    CL=RAD2*AL/(SQRT(RAD2**2-CS**2))
        GO TO 840
  835   CONTINUE
        IF(ICNT .EQ. 2) GO TO 13
        CL=AL*RAD2/(RAD2-R2)
        GO TO 14
  13    CL=RAD2*AL/(SQRT(RAD2**2-R2**I))
  14    CS=R2
```

```
840   Z1=1.0
      SUM=0.0
      TUM=0.0
      NCYCLE=1
      SA=COTAN(SHY)
      IF(NNN .EQ. 1)GO TO 5
      GO TO 6
5     WRITE(6,1111) DS
      WRITE(6,1030)
      WRITE(6,1070)
6     CONTINUE
      DO 210 M=1,2000
      Z=DZ*Z1
      IF(ICNT .EQ. 2) GO TO 15
      DS= DZ*(SQRT(1.+(RAD2/CL)**2))
      RADCI= RAD2*(CL-Z)/CL
      GO TO 16
15    DS=DZ*(SQRT(1.+(RAD2*Z)**2/((CL**2)*(CL**2-Z**2))))
      RADCI=RAD2*(SQRT(CL**2-Z**2))/CL
16    IF(RADCI .LE. R2)GO TO 205
      HC=(-(B2-A2*COTAN(SHY))+SQRT((RADCI/SIN(SHY))**2-(B2*COTAN(SHY)
     1+A2)**2))*((SIN(SHY))**2)
      XC=ARCOS(B2/RADCI)
      BCI=RADCI*SIN(XC)-A2
      IF(BCI .LE. 0.0) BCI=0.0
      ABI=SQRT(HC**2+(HC*COTAN(SHY)+BCI)**2)
      ALAMDA=ARSIN(HC/ABI)
      THETAI=ARSIN(ABI/(2.*RADCI))
      GO TO 220
205   THETAI=ARCOS(DS/RADCI)
      ABI=2.*RADCI*SIN(THETAI)
      HC=ABI*SIN(SHY)
      ALAMDA=SHY
220   DUM=(GAMA*HC**3)*(1.-2.*((COTAN(SHY))**2)+3.*COTAN(ALAMDA)*
     1COTAN(SHY)+3.*COTAN(THETAI)*COTAN(ALAMDA)-3.*COTAN(THETAI)*
     2COTAN(SHY))*DZ/6.
      IF(INDEX .EQ. 2)GO TO 110
      DRM=4.*(RADCI**2)*THETAI*SU*DS
      GO TO 111
110   DRM=CONST*HC*RADCI*(COTAN(ALAMDA)+THETAI*(1.-COTAN(ALAMDA)*
     1COTAN(THETAI)))*DS/(SIN(THETAI)*SIN(ALAMDA))
111   SUM=SUM+DUM
      TUM=TUM+DRM
      Z2=Z+DZ
      Z1=Z1+2.
      DEL=AL-Z2
      IF(DEL .LE.0.01)GO TO 845
      NCYCLE=NCYCLE+1
210   CONTINUE
845   MD=SUM+LC*DM2
      MR=TUM+LC*RM2
850   FS=MR/MD
      RFS=FS/FI2
```

```
      TL=AL+LC
      DELR=RAD2-CS
      RATIC=TL/DELR
      WRITE(6,1040) D,E,FS,RFS,RATIC,NCYCLE,SLM,TLM
      NNN=NNN+1
      IF(E .GE. 3.0E) GO TO 855
      GO TO 810
  855 CONTINUE
      IF(D .GE. 9.0E)GO TO 870
      NK=NK+1
      GO TO 34
  870 CONTINUE
      STOP
      END
C
C     ***************************************************************
C
$IBFTC EGREST
      SUBROUTINE EGREST
C
C                  PLANNER EDGE RESISTING MOMENT
C     ***************************************************************
C
      COMMON/LEV1/ H,SHY,RAD2,A2,B2, SL,DM2,RM2,MD,MR,LC,GLM
      REAL MD,MR,LC
C
C
      GLM=0.0
      AH=H-H/10000.
      AM=COTAN(SHY)
      DN=1
      DY=0.1
      DO 100 LL=1,2000
      Y=DN*DY
      X1=SQRT(RAD2**2-(Y+B2)**2)-A2+Y*AM
      DL=0.1
      TL=1.0
      AX1=X1-X1/10000.
      DO 205 II=1,2000
      XL=TL*DL
      ARM=SQRT((XL+A2-Y*AM)**2+(Y+B2)**2)
      GLM=GLM+4.*DL*DY*ARM*SL
      TL=TL+2.
      XL1=XL+DL
      IF(XL1 .GE. AX1)GO TO 210
  205 CONTINUE
  210 Y1=Y+DY
      DN=DN+2.
      IF(Y1 .GE. AH) GO TO 200
  100 CONTINUE
  200 CONTINUE
      RETURN
      END
```